OPERATOR SPLITTING FOR TWO-PHASE FLOW IN POROUS MEDIA

by

Maryam Khajeh Alijani

A thesis submitted in partial fulfillment of the requirements for the degree of

Master of Science

in

Applied Mathematics

Department of Mathematical and Statistical Sciences
University of Alberta

Abstract

This thesis studies operator splitting for flow equation coupled to a transport equation arising from two-phase (water-oil) model in reservoir simulation. We apply two different types of operator splittings and compare their accuracies. Summarized scheme and alternating triangle method (ATM) in iterative fashion are used in the time discretization. Both schemes are unconditionally stable but the latter is only conditionally consistent. We propose two types of ATM scheme, modified ATM iterative scheme and preconditioned iterative ATM. In the former, we modify the method by adding a correction term to improve the convergence of the modified ATM iterative scheme and the numerical results show that the order of convergence is increased by one. The methods are validated by reporting experimental results for a benchmark data model. Numerical results indicate better accuracy and more reliable solution using summarized scheme compared to ATM schemes.

Preface

This a work of Maryam Khajeh Alijani under the supervision of Peter D. Minev. He proposed the idea of the work and the schemes. I conducted all numerical experiments. To prove the theorem, Peter helped me give the direction by pointing out the relative papers and/or books that can by useful for proving. Then, I used them to prove.

Dedicated to my beloved parents

Acknowledgements

I would like to express my sincere gratitude to my supervisor, Dr. Peter D. Minev. I thank him for his brilliant ideas, tolerance, kindness, financial support and for all the time he spent with me. I admire his integrity, ingenuity and diligence as a researcher and as a person.

I also wish to express my appreciation to Dr. Carolina Diaz-Goano for her invaluable assistance, guidance, and support which built a strong base for my knowledge in reservoir simulation.

A special note of gratitude goes to Dr. Thomas Hillen and Dr. Jochen Kuttler who always were available for providing constructive advise on graduate program.

I would also like to thank my committee members Professor Marc Secanell Gallart, Professor Yau Shu Wong, and Professor Bin Han for their insightful and constructive comments.

I acknowledge the financial support from the Department of Mathematical and Statistical Sciences, University of Alberta. Many thanks to excellent support staff in our department particularly Tara Schuetz and Patty Bobowsky.

Last but not least, special thanks to my parents, Hassan and Fatemeh, my sisters, Leila and Azadeh and my brother, Mohammad for all their prayers, words of encouragement, unconditional love and support throughout my life.

Table of Contents

List of Figures

List of Tables

Chapter 1

Introduction

The main focus of this thesis is to study operator splitting for flow equation, a parabolic equation arising from governing equations of two-phase model in porous media.

The objective of reservoir engineering is to optimize the recovery of oil. To achieve this, one should predict the performance of reservoir under various exploitation schemes, especially when enhanced oil recovery or recovery from heavy oil is considered. This requires the use of numerical techniques to solve the mathematical equations of flows in oil reservoirs. Also, simulation technology has undergone dramatic development due to availability of computing power and sophistication of simulation techniques such as the rapid advance of parallel computers and algorithms corresponding to them. This availability will let fast and efficient approximation of the solution of complex nonlinear system of partial differential equations (PDEs) involved in the modelling of oil reservoir to be possible.

There are several challenges to an efficient scalable reservoir simulator. Firstly, the governing PDEs are coupled hyperbolic-parabolic equations due

to coupling between the flow (pressure) and the transport (phase saturations) problems. Secondly, the rock properties such as porosity and permeability exhibit high spatial variation of scales in heavy and extra heavy oil field in Alberta which affects oil production significantly [8]. This leads to a huge computational problem and its solution is infeasible even on large parallel computers. Finally, fluid velocities vary rapidly over the domain, with near well regions having fast flows and far away regions almost no flow [10].

Since easy-to-produce oil fields are gone and there are lots of bitumen resources, oil industry has been motivated to do innovation and integrated approaches to produce oil from the existing reservoirs (deep-water offshore, oil sands and heavy oil). Examples of those innovations in enhanced oil recovery are: 1) chemical injection, 2) thermal recovery (Cyclic Steam Stimulation (CSS), Steam Flooding, Steam Assisted Gravity Drainage (SAGD), and in-situ combustion). To optimize the production and minimize the risk of associated recovery methods, the oil industry use numerical simulations which is relatively inexpensive and the simulation results become as an indispensable tool in nearly all major reservoir development decisions [10].

1.1 Thesis Outline

The thesis is formed of seven chapters.

Chapter one provides a brief introduction regarding reservoir simulation and its numerical challenges.

In chapter two, we have a literature review on reservoir simulation and explain the impact of this thesis. We then introduce governing equation for a compositional model for three components and three phases together with

well equations. Then, we reduce that model into a two-phase (water-oil) model and discuss its nondimensionalization.

Chapter three deals with time and space approximation. For temporal discretization, we discuss linearization approach, explicit approach and two different types of operator splitting schemes, summarized scheme and alternating triangle method will be introduced. To improve the accuracy, we propose a preconditioned iterative scheme based on summarized scheme. We also devise two variants of alternating triangle method, modified iterative alternating triangle method and preconditioned iterative alternating triangle method. Then, depending on the well constraint we show how the well equations will be coupled to the splitting schemes. Next, spatial discretization is presented in which we use finite volume discretization. We also explain the first order single-point upstream approximation for discretization of relative permeability.

We focus on the stability of both proposed splitting schemes in chapter four. We show that summarized scheme is unconditionally stable for non-negative directional operators following the work of Vabishchevich in [23]. The unconditionally stability of alternating triangle method will be shown in the framework of Vabishchevich in [24].

Chapter five presents the error analysis. This is done in the framework of Vabishchevich in [23, 24]. By applying the stability results in chapter four, it follows the convergence estimates.

Numerical results are illustrated in chapter six. We compare the accuracy of the schemes and their order of convergence. Time history of the numerical solutions for the splitting schemes is also presented in which the numerical results of the schemes are compared to a reference solution.

In chapter seven, we propose next phase of our work. We introduce a new

splitting scheme proposed by Vabishchevich in [22]. This splitting scheme is obtained naturally from the flow equation by taking flux as a new variable. A detailed discussion of this scheme including temporal and spatial discretization will be presented.

Chapter 2

Governing Equations

In general, governing equations of a mathematical model of a reservoir cannot be solved by analytical methods. Instead, a numerical method may be produced to approximate the solution by computers [2]. The books by [14] and [1] gave detailed information on the use of finite difference methods as applied to the porous media flow. Compared with finite difference methods, finite element methods when applied to petroleum reservoir simulation have the following features: such as in the reduction of grid orientation effect, in the treatment of local grid refinement, horizontal and slanted wells, in the simulation of faults and fractures and in the requirement of high-order accuracy of numerical solutions [2].

Two variations of finite element methods, Control volume finite element methods and discontinuous finite element methods posses a local mass conservation property on each control volume. The finite difference methods are also locally conservative [2].

A basic scheme for solving multiphase flow equations is simultaneous solution (SS) method. It solves all of the coupled nonlinear equations simultane-

ously and implicitly. This method is stable and for the black oil and thermal models with a few components is a good choice. However, for compositional and chemical compositional flow problems with many compositional components the size of system matrices is too large that even with today's computing power it becomes computationally expensive [2]. A variation without suffering too much in computation with less stability is the Implicit Pressure Explicit Saturation (IMPES) scheme. This scheme works well for problems of intermediate difficulty and nonlinearity e.g. two-phase incompressible flow. However, it is not sufficient for problems with strong nonlinearity, especially for problems with more than two phases. Different sequential methods for solving equations in an implicit fashion without a full coupling have been developed. They are more computationally efficient but less stable than SS method and more stable but less efficient than IMPES scheme. They are suitable for compositional and chemical compositional flow problems with many chemical components. The last method which can be used in reservoir simulation is an adaptive implicit scheme. The idea of this scheme is to find an efficient middle method between the IMPES or sequential and SS schemes. That means it only apply the expensive SS scheme to those gridblocks that require it and on the remaining gridblocks the IMPES scheme is applied [2].

In this thesis, our reservoir model is a two-phase incompressible flow so we implement our simulation using IMPES scheme. However, this scheme still suffer computationally from implicit discretization of pressure equation especially on large grids for 3D problems. To overcome this problem, we decompose the spatial operator in pressure equation while stability is maintained. The main contribution of this thesis is that we develop a stable, efficient, robust and accurate solution technique based on direction splitting method that ad-

dresses the first challenge in chapter 1. To address the second challenge, we propose an innovative algorithm in section 7.2 to handle the dramatic changes appeared in permeability data. The algorithm uses flux-splitting scheme which leads to a construction of multi-sale method.

In the following, we introduce the governing equations. Compositional models of reservoir assume at most three phases (water, oil, and gas) and several hydrocarbon components while diffusive effects are neglected. In the SAGD model, we consider three components: H2O ($i = 1$), Bitumen ($i = 2$), Methane ($i = 3$).

Let ϕ and K denote the porosity and permeability of the porous medium $\Omega \subset \mathbb{R}^3$, and let S_α, μ_α, u_α, $k_{r\alpha}$, and ρ_α to be the saturation, viscosity of fluid, volumetric velocity, relative permeability and density of phase α for $\alpha \in \{\text{water, oil, gas}\}$ denoted as w, o, g respectively. Also, $c_{i\alpha}$ is the mass fraction of the ith component in phase α and q_α is the flow rate of phase α.

The governing equations for multiphase compositional flow are based on the conservation of mass for each component. We assume that the water component can exist in both aqueous (water) phase and vapour (gas) phase and the oil component exist only in the liquid hydrocarbon (oil) phase and the gas component can exist in both the liquid and vapour hydrocarbon (oil and gas) phases. For the sake of simplicity, we also assume that all phases have the same pressure so capillary pressure does not exist. With these assumptions the mass balance equations take the following form [9]:

$$\frac{\partial}{\partial t}\left(\phi \sum_{\alpha=w}^{g} S_\alpha \rho_\alpha c_{i\alpha}\right) = -\nabla\cdot\left(\sum_{\alpha=w}^{g} u_\alpha \rho_\alpha c_{i\alpha}\right) + \sum_{\alpha=w}^{g} c_{i\alpha}\rho_\alpha q_\alpha, \quad i = 1, 2, 3, \tag{2.1}$$

where the superficial velocity u_α is given by momentum conservation per phase

α in the form of Darcy's law as:

$$u_\alpha = -\frac{1}{\mu_\alpha}\left(K\ k_{r\alpha}\nabla\Phi_\alpha\right), \qquad \alpha = w, o, g, \tag{2.2}$$

Φ_α stands for potential of phase α with $\nabla\Phi_\alpha = \nabla P + \wp\rho_\alpha\nabla z$ in which P is pressure, $\wp$ is gravitational acceleration, and z is depth.

In the case of non-isothermal flows, an energy conservation equation is supplemented which takes the following form [2]:

$$\frac{\partial}{\partial t}\left(\phi\sum_{\alpha=w}^{g} S_\alpha\rho_\alpha U_\alpha + (1-\phi)\rho\ C_p\ T\right) = \nabla\cdot\left(k_t\ \nabla T\right) - \nabla\cdot\left(\sum_{\alpha=w}^{g} u_\alpha\rho_\alpha H_\alpha\right) + q_c - q_L \tag{2.3}$$

where U_α is internal energy of fluid in phase α, ρ is constant density at reference condition, C_p is heat capacity of solid, T is temperature, k_t is average thermal conductivity, H_α is enthalpy of phase α, q_c denotes the heat source item, and q_L indicates the heat loss to overburden and underburden.

In addition to differential equations (2.1) and (2.3), there are the following algebraic constraints. Since the pore space is saturated, we have saturation constraint:

$$\sum_{\alpha=w}^{g} S_\alpha = 1, \qquad \alpha = w, o, g, \tag{2.4}$$

and the mole fraction balance implies that [2]:

$$x_{1w} = 1, \tag{2.5}$$

$$x_{2o} + x_{3o} = 1, \tag{2.6}$$

$$x_{1g} + x_{3g} = 1, \tag{2.7}$$

where $x_{i\alpha}$, is mole fraction of the ith component in the phase α.

One of the mathematical techniques to handle the distribution of chemical components among phases is Equilibrium K-values. Since mass interchange between phases occurs much faster than the flow of porous media fluids, it is physically reasonable to assume that the phases to be in the phase equilibrium state. The equilibrium ratio for component $i = 1$ and $i = 3$ are defined as [4]:

$$K_1(P,T) = \frac{x_{1g}}{x_{1w}}, \tag{2.8}$$

$$K_3(P,T) = \frac{x_{3g}}{x_{3o}}. \tag{2.9}$$

In practical simulations, we rewrite PDEs in terms of a set of independent primary variables. For example, one can choose P, S_o, S_g, and T as primary variables and then use the algebraic equations (2.4)-(2.9) to calculate the remaining variables.

The system of PDEs is supplemented with zero flux boundary conditions:

$$\left(\sum_{\alpha=w}^{g} \mathrm{u}_\alpha \rho_\alpha c_{i\alpha}\right) \mathbf{.n} = 0, \quad \text{on} \quad \partial\Omega \quad \text{for} \quad \text{i=1, 2, 3,}$$

where $\mathbf{n}$ denotes the outward normal unit vector to the boundary. The initial

conditions are

$$P(x,0) = P_0(x),$$
$$S_w(x,0) = S_{w0}(x),$$
$$S_g(x,0) = S_{g0}(x),$$
$$T(x,0) = T_0(x).$$

2.1 Sink/Source well model

Well controls or operation constraints are the values used to determine operation of the wells [5]. There are several well constraints to be considered in injector and producer wells. For injection well, there are usually two kinds of constraints, either maximum wellbore pressure (known as well bottom hole pressure, P_{bh}) is given or an injection rate is known. For production well, there are three kinds of well constraints. Minimum bottom hole pressure, constant total liquid (water and oil) production rate, and a constant total rate [2].

The flow rates at the wells are given by [2, 15]:

$$q_\alpha = \sum_{j=1}^{N_w} \sum_{m=1}^{M_{wj}} WI^{(j,m)} \lambda_\alpha \left[P_{bh}^{(j)} - P - \rho_\alpha \wp \left(z_{bh}^{(j)} - z \right) \right] \delta(\boldsymbol{x} - \boldsymbol{x}^{(j,m)}), \qquad (2.10)$$

where $\delta(x)$ is the Dirac-delta function, N_w is the total number of wells, M_{wj} is the total number of perforated zones of the jth well, and $x^{(j,m)}$ is central location of the mth perforated zone of the jth well, P_{bh}^{j} is the bottom hole pressure of the jth well at the well datum z_{bh}, $WI^{(j,m)}$ denotes well index and

has the form:

$$WI^{(j,m)} = \frac{2\pi \bar{K} \Delta L^{(j,m)}}{\ln\left(r_e^{(j,m)}/r_w^j\right) + S}, \tag{2.11}$$

in which $\Delta L^{(j,m)}$ is the grid length, $\bar{K}$ is an average of K at the wells, r_w^j denotes the wellbore radius of the jth well, $r_e^{(j,m)}$ is the drainage radius of the jth well at the gridblock in which $x^{(j,m)}$ is located, and S is skin factor.

2.2 Two-phase (water-oil) model

Depending on the stage of oil recovery, the fluids filling a reservoir will change. At primary stage, the reservoir mainly consists of single fluid such as gas or oil. At this stage, oil or gas production is done through simple natural decompression at the wells. This stage is called primary recovery and it can recover 20–30% of hydrocarbons from the oil field. In order to recover the rest of remaining oil, a fluid (usually water) is injected into the injector well and oil is produced from the producer well. This process keeps the reservoir pressure and flow rates high resulting in displacement of some of the oil toward the production well. This stage is known as secondary recovery or water flooding stage. At this stage, if reservoir pressure is greater than the bubble point pressure (pressure at which the flow of fluids consists of only water and oil and no free gas is present meaning all the gas is in solution) then there is two-phase immiscible flow. The water phase that wets the porous medium more than the other phase i.e. oil is called wetting phase and oil phase is called non-wetting phase. There is no mass interchange between these two phases [2].

We describe the governing differential equations for two-phase incompressible immiscible flow in a porous medium Ω. The mass conservation law for

each phase $\alpha = w, o$ using (2.1) is:

$$\frac{\partial}{\partial t}\left(\phi(P)\ S_\alpha(t)\ \rho_\alpha(P)\right) = \nabla\cdot\left(K(\boldsymbol{x})\ \frac{k_{r\alpha}(S_\alpha(t))}{\mu_\alpha}\ \nabla\Phi_\alpha(P)\ \rho_\alpha(P)\right) + \rho_\alpha(P)\ q_\alpha(P, S_\alpha), \qquad \alpha = w, o, \tag{2.12}$$

where $\nabla\Phi_\alpha = \nabla P + \wp\rho_\alpha\nabla z$, for $\alpha = w, o$. Filling the void spaces by the two fluids implies that

$$S_w + S_o = 1. \tag{2.13}$$

With incompressibility assumption densities and porosity are constant [2]. We divide each equation in (2.12) by ρ_α and add them up to derive pressure equation:

$$\phi\ \frac{\partial}{\partial t}\left(S_w + S_o\right) = \nabla\cdot\left(K\ \frac{k_{rw}}{\mu_w}\ \nabla\Phi_w + K\ \frac{k_{ro}}{\mu_o}\ \nabla\Phi_o\right) + q_w + q_o, \tag{2.14}$$

using (2.13), we get a stationary equation (elliptic equation) for pressure:

$$0 = \nabla\cdot\left(K\ \frac{k_{rw}}{\mu_w}\ \nabla\Phi_w + K\ \frac{k_{ro}}{\mu_o}\ \nabla\Phi_o\right) + q_w + q_o. \tag{2.15}$$

In order to get a parabolic equation for pressure, we assume slight compressibility for porosity i.e. $\phi = \phi(P)$ while densities are still constant. Dividing each equation in (2.12) by ρ_α and adding them up yields:

$$\phi\ \frac{\partial}{\partial t}\left(S_w + S_o\right) + \frac{\partial\phi}{\partial t}\ \left(S_w + S_o\right) = \nabla\cdot\left(K\ \frac{k_{rw}}{\mu_w}\ \nabla\Phi_w + K\ \frac{k_{ro}}{\mu_o}\ \nabla\Phi_o\right) + q_w + q_o, \tag{2.16}$$

applying (2.13), we get a parabolic equation for pressure:

$$\frac{\partial \phi}{\partial P}\,\frac{\partial P}{\partial t} = \nabla\cdot\left(K\,\frac{k_{rw}}{\mu_w}\,\nabla\Phi_w + K\,\frac{k_{ro}}{\mu_o}\,\nabla\Phi_o\right) + q_w + q_o. \tag{2.17}$$

We set $C = \dfrac{\partial \phi}{\partial P}$ where C corresponds to the compressibility of the rock. Thus, pressure equation reads as the following:

$$C\,\frac{\partial P}{\partial t} = \nabla\cdot\left(K\,\frac{k_{rw}}{\mu_w}\,\nabla\Phi_w + K\,\frac{k_{ro}}{\mu_o}\,\nabla\Phi_o\right) + q_w + q_o. \tag{2.18}$$

Saturation equation for water phase is obtained from (2.12) by diving it by ρ_w:

$$\phi\frac{\partial S_w}{\partial t} = \nabla\cdot\left(K\,\frac{k_{rw}}{\mu_w}\,\nabla\Phi_w\right) + q_w. \tag{2.19}$$

Equations (2.13), (2.18), and (2.19) provide three equations for three unknown P, S_w, and S_o. We choose to solve for primary unknowns P and S_w.

We present the unit of all variables and parameters appearing in the two-phase mass balance equations, Darcy's law and well equation in table 2.1 before we discuss nondimensionalization in the next section.

Table 2.1: Variables and parameters used in two-phase model mass balance equations, Darcy's law and well equation

Symbol	Quantity	Metric Unit
x, y, z	Length	m
K	Permeability	μm^2
P	Pressure	kPa
P_{bh}	Bottom hole pressure	kPa
Φ_α	Phase potential	kPa
μ_α	Phase viscosity	$Pa.s$
ρ_α	Phase density	$\frac{Kg}{m^3}$
u_α	Phase velocity	$\frac{m}{s}$
q_w	Water flow rate	$\frac{1}{day}$
q_o	Oil flow rate	$\frac{1}{day}$
$\wp$	Gravitational acceleration	$\frac{m}{s^2}$
C	Compressibility	kPa^{-1}
$k_{r\alpha}$	Phase relative permeability	dimensionless(fraction)
ϕ	Porosity	dimensionless(fraction)
S_α	Phase saturation	dimensionless(fraction)
t	Time	day
WI	Well index	m^3
r_e	Effective block radius	m
r_w	Wellbore radius	m
S	Skin factor	dimensionless
CC	Geometric factor	dimensionless
f	Well fraction	dimensionless

2.3 Nondimensionalization

Using mathematical symbols when dealing with differential equations with pen and paper, it does not matter what units and numerical values we use for a physical parameter. However, units become important while doing numerical simulations, hence dealing with approximations and errors. Nondimensionalization of mathematical models is a very useful technique which has great practical benefits relating to running numerical simulations. There are three main purposes for scaling. First, instead of letting very small or very large input quantities enter the computations, scaling makes the size of independent and dependent variables of unit size. Second, in the scaled model the independent and dependent variables are dimensionless and the final purpose is that the number of parameters in the scaled model are less than the number of physical parameters in the original model [11]. All of these benefits motivate us to do nondimensionalization. We introduce the following dimensionless fractions of water and oil fluid properties [11]:

$$\rho = \rho_w,\ \rho_o = \rho\alpha,\ \alpha = \frac{\rho_o}{\rho_w},$$
$$\mu = \mu_w,\ \mu_o = \mu\beta,\ \beta = \frac{\mu_o}{\mu_w},$$
$$q = q_w,\ q_o = q\omega,\ \omega = \frac{q_o}{q_w}.$$

We also make the following quantities dimensionless by choosing new variables. Dimensionless variables are indicated by bar:

$$
\begin{aligned}
&\bar{K} = \frac{K(\boldsymbol{x})}{K_c}, && K_c = \max_{\boldsymbol{x}} K(\boldsymbol{x}),\\
&\Lambda_w = K\frac{k_{rw}}{\mu_w} = \Lambda_c\bar{\Lambda}_w, && \Lambda_c = \frac{K_c}{\mu}, \quad \bar{\Lambda}_w = \bar{K}k_{rw},\\
&\Lambda_o = K\frac{k_{ro}}{\mu_o} = \Lambda_c\beta^{-1}\bar{\Lambda}_o, && \bar{\Lambda}_o = \bar{K}k_{ro},\\
&\Lambda_t = \Lambda_w + \Lambda_o = \Lambda_c\bar{\Lambda}_t, && \bar{\Lambda}_t = \bar{\Lambda}_w + \beta^{-1}\bar{\Lambda}_o,\\
&\bar{x} = \frac{x}{L_c}, && \bar{P} = \frac{P}{P_c}, \quad \bar{v} = \frac{v}{v_c},\\
&t_c = \frac{L_c}{v_c}, && \bar{t} = \frac{t}{t_c}.
\end{aligned}
$$

We choose a characteristic length L_c while natural velocity scale is obtained by pressure term in Darcy's law with $v_c = \dfrac{K_cP_c}{\mu L_c} = \dfrac{\Lambda_cP_c}{L_c}$ and P_c represents characteristic pressure. The derivative relations are,

$$
\frac{\partial}{\partial t} = \frac{1}{t_c}\frac{\partial}{\partial \bar{t}} \quad \text{and} \quad \nabla := \left(\frac{\partial}{\partial x}, \frac{\partial}{\partial y}, \frac{\partial}{\partial z}\right) = \frac{1}{L_c}\left(\frac{\partial}{\partial \bar{x}}, \frac{\partial}{\partial \bar{y}}, \frac{\partial}{\partial \bar{z}}\right) = \frac{1}{L_c}\bar{\nabla}.
$$

S_w, S_o, k_{rw}, k_{ro}, and ϕ are non-dimensional quantities. We insert the above scaled quantities in (2.18) and (2.19) to get:

$$
\frac{\partial \bar{P}}{\partial \bar{t}} = \frac{1}{CP_c}\bar{\nabla}\cdot\left(\bar{\Lambda}_t\bar{\nabla}\bar{P}\right) + \frac{\rho_{\wp}L_c}{P_c^2C}\,\bar{\nabla}\cdot\left((\bar{\Lambda}_w + \beta^{-1}\alpha\bar{\Lambda}_o)\bar{\nabla}\bar{z}\right) + \frac{t_c}{CP_c}\left(q + q\omega\right), \tag{2.20}
$$

$$
\phi\frac{\partial S_w}{\partial \bar{t}} = \bar{\nabla}\cdot\left(\bar{\Lambda}_w\bar{\nabla}\bar{P}\right) + \frac{t_c\Lambda_c\rho_{\wp}}{L_c}\,\bar{\nabla}\cdot\left(\bar{\Lambda}_w\bar{\nabla}\bar{z}\right) + t_cq. \tag{2.21}
$$

Introducing other dimensionless numbers $\eta = \dfrac{\rho_{\wp}L_c}{P_c} = \dfrac{t_c\Lambda_c\rho_{\wp}}{L_c}$, and $\zeta = t_cq$, we can rewrite (2.20) and (2.21) in the following final dimensionless equations:

$$
\frac{\partial \bar{P}}{\partial \bar{t}} = \frac{1}{CP_c}\bar{\nabla}\cdot\left(\bar{\Lambda}_t\bar{\nabla}\bar{P}\right) + \frac{\eta}{CP_c}\bar{\nabla}\cdot\left((\bar{\Lambda}_w + \beta^{-1}\alpha\bar{\Lambda}_o)\bar{\nabla}\bar{z}\right) + \frac{\zeta(1+\omega)}{CP_c}, \tag{2.22}
$$

$$\phi\frac{\partial S_w}{\partial \bar{t}} = \bar{\nabla}\cdot\left(\bar{\Lambda}_w\bar{\nabla}\bar{P}\right) + \eta\bar{\nabla}\cdot\left(\bar{\Lambda}_w\bar{\nabla}\bar{z}\right) + \zeta. \tag{2.23}$$

By doing the nondimensionalization, we reduce eight parameters L_c, q_w, q_o, $\mu_w, \mu_o, \rho_w, \rho_o$, and K to five dimensionless parameters $\alpha, \beta, \omega, \eta$, and ζ. We now drop the bar from the nondimensionalized variables for the sake of simplicity to get the nondimensionalized equations that we will solve:

$$\frac{\partial P}{\partial t} = \frac{1}{CP_c}\nabla\cdot(\Lambda_t\nabla P) + \frac{\eta}{CP_c}\nabla\cdot\left((\Lambda_w + \beta^{-1}\alpha\Lambda_o)\nabla z\right) + \frac{\zeta(1+\omega)}{CP_c}, \tag{2.24}$$

$$\phi\frac{\partial S_w}{\partial t} = \nabla\cdot(\Lambda_w\nabla P) + \eta\nabla\cdot(\Lambda_w\nabla z) + \zeta. \tag{2.25}$$

Water rate, q_w, for two-phase model for single point well located at i-th perforated grid in the vertical direction from (2.10) is defined as:

$$q_w = WI\ \frac{k_{rw}}{\mu_w}\ (P_{bh} - P)\ \frac{1}{\Delta x\ \Delta y\ \Delta z}\ \delta(\boldsymbol{x} - \boldsymbol{x}^i), \tag{2.26}$$

with anisotropic permeability $K = \mathrm{diag}(K_{11}, K_{22}, K_{33})$, (2.11) reduces to

$$WI = \frac{2\pi\sqrt{K_{11}K_{22}}\ \Delta z}{\ln(r_e/r_w) + S},$$

where Δz is the grid length and effective block radius, r_e, is given by:

$$r_e = \frac{2\ CC\sqrt{\sqrt{K_{22}/K_{11}}\Delta x^2 + \sqrt{K_{11}/K_{22}}\Delta y^2}}{\left((K_{22}/K_{11})^{0.25} + (K_{11}/K_{22})^{0.25}\right)\sqrt{\pi f}},$$

in which CC denotes geometric factor. The geometric factor depends on the geometry of the problem. f is well fraction that will be 1 for a well going approximately through the centre of a grid block, $\frac{1}{2}$ for a half well on a grid block boundary, and $\frac{1}{4}$ for a quarter well at the corner of a grid block [4].

Inserting scaled quantities into (2.26) we get:

$$\bar{q}_w = \bar{WI}\ \frac{k_{rw}}{\mu}\ P_c\ (\bar{P_{bh}} - \bar{P})\ \frac{1}{L_c^3}\ \delta(\bar{\boldsymbol{x}} - \bar{\boldsymbol{x}}^i). \tag{2.27}$$

We denote,

$$\bar{P_{bh}} = \frac{P_{bh}}{P_c},$$

$$\bar{WI} = \frac{2\pi\ K_c L_c\ \sqrt{\bar{K}_{11}\bar{K}_{22}}\ \bar{\Delta z}}{\ln(\bar{r_e}/r_w) + S},$$

$$\bar{r_e} = \frac{2\ CC\ L_c\ \sqrt{\sqrt{\bar{K}_{22}/\bar{K}_{11}}\bar{\Delta x}^2 + \sqrt{\bar{K}_{11}/\bar{K}_{22}}\bar{\Delta y}^2}}{\left((\bar{K}_{22}/\bar{K}_{11})^{0.25} + (\bar{K}_{11}/\bar{K}_{22})^{0.25}\right)\sqrt{\pi f}},$$

$$\bar{\Delta x} = \frac{\Delta x}{L_c}, \quad \bar{\Delta y} = \frac{\Delta y}{L_c}, \quad \bar{\Delta z} = \frac{\Delta z}{L_c},$$

$$\bar{K}_{ii} = \frac{K_{ii}}{K_c}, \quad i = 1, 2, 3.$$

Dropping the bar, we get:

$$q_w = WI\ \frac{k_{rw}}{\mu}\ P_c\ (P_{bh} - P)\ \frac{1}{L_c^3}\ \delta(\boldsymbol{x} - \boldsymbol{x}^i). \tag{2.28}$$

In the same way as explained above, the scaled volumetric rate, q_o, for oil phase can be obtained:

$$q_o = WI\ \frac{k_{ro}}{\mu\beta}\ P_c\ (P_{bh} - P)\ \frac{1}{L_c^3}\ \delta(\boldsymbol{x} - \boldsymbol{x}^i). \tag{2.29}$$

Chapter 3

Discrete Approximation

Majority of reservoir simulators used (and still use) finite volume methods of discretization for the multiphase flow equations and this choice is motivated by the need for exact local conservation [10]. The system of PDEs are quite large and nonlinear with coupled parabolic and hyperbolic equations. Thus, the choice of solution technique is a major issue. Fully implicit simultaneous solution technique (SS) together with finite volume/finite element yields a nonlinear system that is linearized with Newton-Raphson method but the resulting spatial discretization is very expensive to be solved for compositional type of flow due to the number of chemical component. IMPES and sequential techniques are widely used in petroleum industry [2]. An IMPES method was originally developed by Sheldon et al. [17] and Stone and Garder [21]. The basic idea of this classical method for solving (2.12) is to separate the computation of pressure from that of saturation. That is, the coupled system is split into a pressure equation (2.24) and a saturation equation (2.25), and the pressure and saturation equations are solved using implicit and explicit time approximation approaches, respectively. This method is simple to set

up and efficient in implementation, and requires less computer memory than other methods such as the SS method (Douglas et al. [6]). Although explicit treatment of saturation requires small time steps for the saturation equation to be stable, IMPES is still popular in the petroleum industry and a very powerful method for solving two-phase flow particularly for incompressible or slightly compressible fluids [2].

3.1 Temporal Discretization

3.1.1 Linearization Approach

We will discretize equations (2.24) and (2.25) in time. We divide the time interval $[0, T]$ into N equidistance time step τ and let $t^n = n\tau, n = 0, 1, \cdots N$ and denote approximation of $\mathsf{P}(t^n)$, $\mathsf{S}_w(t^n)$ and $\mathsf{S}_o(t^n)$ by P^n, S_w^n, and S_o^n respectively. We rewrite equation (2.24) as:

$$\frac{\partial \mathsf{P}}{\partial t} = \frac{1}{CP_c}\nabla\cdot(\Lambda_t \nabla \mathsf{P}) + f, \quad (\boldsymbol{x}, t) \in \Omega \times \mathbb{R}^+ \tag{3.1}$$

where

$$f = \frac{\eta}{CP_c}\nabla\cdot\left((\Lambda_w + \beta^{-1}\alpha\Lambda_o)\nabla z\right) + \frac{\zeta(1+\omega)}{CP_c}.$$

In the linearization approach for equation (3.1), we use explicit treatment for saturation dependent variables while evaluating pressure at the current time level as follows:

$$\frac{P^{n+1} - P^n}{\tau} = \frac{1}{CP_c}\nabla\cdot\Big(\Lambda_t(S_w^n, S_o^n)\ \nabla P^{n+1}\Big) + f^{n+1}, \tag{3.2}$$

where

$$f^{n+1} = \frac{\eta}{CP_c}\nabla.\Big((\Lambda_w^n + \beta^{-1}\alpha\Lambda_o^n)\nabla z\Big) + \frac{\zeta^{n+1}(1+\omega^{n+1})}{CP_c}, \tag{3.3}$$

is an approximation to $f(\mathsf{P}(t^{n+1}), \mathsf{S}_w(t^n), \mathsf{S}_o(t^n))$. The source/sink term which appears in f needs spacial consideration due to the type of the constraint of well and we will discuss it in details later. The problem (3.2) reduces to solving the implicit reaction-diffusion equation:

$$\left(I - \frac{\tau}{CP_c}\nabla.(\Lambda_t^n\nabla)\right)\frac{P^{n+1}}{\tau} = \frac{P^n}{\tau} + f^{n+1}. \tag{3.4}$$

Implicit approximation (3.4) is unconditionally stable but requires computing $\left(I - \frac{\tau}{CP_c}\nabla.(\Lambda_t^n\nabla)\right)^{-1}\left(\frac{P^n}{\tau} + f^{n+1}\right)$, which is computationally expensive for three-dimensional problems on very large grids, and hence iterative solvers for sparse matrices need to be used. To reduce computational cost for parabolic equations of second order, explicit schemes or different variant of operator-splitting schemes are employed [12, 25].

3.1.2 Explicit-time Integration

Explicit schemes have implementation advantages over implicit schemes. However they have the severe restrictions on time step sizes. For the parabolic equations, the stability restriction is $\tau < \mathcal{O}(h^2)$, where h denotes grid size [19, 20].

Explicit discretization of saturation equation (2.25), which is also called

the forward difference scheme, when P^{n+1} is known, results in:

$$\phi\frac{S_w^{n+1}-S_w^n}{\tau} = \nabla\cdot\Big(\Lambda_w(S_w^n)\nabla P^{n+1}\Big) + \eta\nabla\cdot\Big(\Lambda_w(S_w^n)\nabla z\Big) + \zeta\left(P^{n+1}, S_w^n\right). \tag{3.5}$$

This scheme is only conditionally stable, that is, the time step must satisfy the stability condition. We derive the stability condition in section 3.3.

3.1.3 Operator Splitting Methods

Since most of computational time in IMPES method is spent on the implementation of implicit calculation of pressure, it is reasonable to find an alternative way which is computationally cheaper while having unconditionally stable property. In direction splitting methods, a spatial operator is represented as sum of one-dimensional operators so the original problem is decomposed into a sequence of one-dimensional implicit discrete problems. Time discretization of the one-dimensional problem leads to a tridiagonal matrix in which direct solver can be applied. Let us decompose the spatial operator A from the equation (3.1),

$$A = -\frac{\partial}{\partial x}\Big(\frac{\Lambda_t(\boldsymbol{x},t)}{CP_c}\frac{\partial}{\partial x}\Big) - \frac{\partial}{\partial y}\Big(\frac{\Lambda_t(\boldsymbol{x},t)}{CP_c}\frac{\partial}{\partial y}\Big),$$

into the sum of two operators in 2D (and into the sum of three operators in 3D):

$$A_1 = -\frac{\partial}{\partial x}\Big(\frac{\Lambda_t(\boldsymbol{x},t)}{CP_c}\frac{\partial}{\partial x}\Big),$$

$$A_2 = -\frac{\partial}{\partial y}\Big(\frac{\Lambda_t(\boldsymbol{x},t)}{CP_c}\frac{\partial}{\partial y}\Big),$$

so that

$$A = A_1 + A_2.$$

We substittute the introduced operators into (3.1) and we obtain the Cauchy problem of finding $\mathsf{P}(t)$ such that,

$$\begin{aligned} &\frac{\partial \mathsf{P}}{\partial t} + A\mathsf{P} = f, \quad t > 0 \\ &\mathsf{P}(0) = \mathsf{P}_0. \end{aligned} \tag{3.6}$$

We rewrite equation (3.2) as:

$$\frac{P^{n+1} - P^n}{\tau} + A\ P^{n+1} = f^{n+1}, \tag{3.7}$$

which can be written as operator equation:

$$(I + \tau A)P^{n+1} = P^n + \tau f^{n+1}. \tag{3.8}$$

There is a variety of schemes that can be used to approximate the solution of a parabolic problem by first decomposing the elliptic operator into a sum of positive operators and then solving a set of parabolic subproblems. Here, we consider an easy scheme that is unconditionally stable for non-commutative decomposition and it is only first order accurate in time. We consider the so-called "summarized approximation" that is known as "Marchuk-Yanenko splitting". The summarized scheme in 2D is defined by the two-component additive splitting $A = A_1 + A_2 \geq 0$ with A_1 and A_2 to be defined as above [23]. The splitting scheme reads as follows: starting from $P^0 = \mathsf{P}_0$, we solve the following set of d subproblems (supposedly easier problems) for intermediate

unknowns $P^{n+\alpha/d},\ \alpha = 1, \cdots, d$ such that after d sub-steps, we get P^{n+1}, an approximated solution to the problem (3.6),

$$\frac{P^{n+\alpha/d} - P^{n+(\alpha-1)/d}}{\tau} + A_\alpha(\sigma_\alpha P^{n+\alpha/d} + (1-\sigma_\alpha)P^{n+(\alpha-1)/d}) = q^{n+1,\alpha}.$$

Here $\sum_{\alpha=1}^{d} q^{n+1,\alpha} = f^{n+1}$ is some approximation to $f(t^{n+1}, \boldsymbol{x})$. In our model, $d = 2$ and we set σ_α =1 which results in the implicit scheme for each subproblem as:

$$\begin{aligned} \frac{P^{n+1/2} - P^n}{\tau} + A_1^n P^{n+1/2} &= q^{n+1,1}, \\ \frac{P^{n+1} - P^{n+1/2}}{\tau} + A_2^n P^{n+1} &= q^{n+1,2}. \end{aligned} \tag{3.9}$$

If we set $q^{n+1,1} = f^{n+1}$ and $q^{n+1,2} = 0$, still $q^{n+1,1} + q^{n+1,2} = f^{n+1}$ holds. This helps eliminate $P^{n+1/2}$ from (3.9) and rewrite it in the factorized form:

$$(I + \tau A_1)(I + \tau A_2)P^{n+1} = P^n + \tau f^{n+1}. \tag{3.10}$$

We devise a preconditioned iterative method for equation (3.8) based on the summarized scheme (3.10) as follows:

$$\begin{aligned} (I + \tau A_1)(I + \tau A_2)(P^{n+1,k+1} - P^{n+1,k}) = (P^n + \tau f(P^{n+1,k}, S_w^n, S_o^n)) \\ - (I + \tau A)P^{n+1,k}. \end{aligned} \tag{3.11}$$

For the design of the preconditioner $(I + \tau A_1)(I + \tau A_2)$, we take into account two main requirements: the preconditioner is chosen so as to be easily invertible on one hand, and on the other hand, to "resemble" the

problem operator $(I + \tau A)$. This means we can expect that the operator $((I + \tau A_1)(I + \tau A_2))^{-1}(I + \tau A)$ will "resemble" the unit operator I, and the boundaries of its spectrum λ_{min} and λ_{max}, as well as the condition number, will all be "close" to one. We note that the right-hand side of (3.11) is the residual of (3.8) and k denotes the iteration parameter.

In the following, we discuss other splitting method that employ splitting into lower and upper triangular discrete operators.

The Alternating Triangle Method (ATM) as presented by Smarskii in [18, 19] is defined by the two-component additive splitting,

$$\mathcal{A} = \mathcal{A}_1 + \mathcal{A}_2 \geq 0,$$

where $\mathcal{A}$ is the discrete operator for the operator A and the two operators $\mathcal{A}_1$ and $\mathcal{A}_2$ are adjoint to each other, i.e.,

$$\mathcal{A}_1^* = \mathcal{A}_2.$$

The elements of the matrices $\mathcal{A}_\alpha = \{a_{ij}^\alpha\}, \alpha = 1, 2$, using the notation in [23], are as follows,

$$a_{ij}^1 = \begin{cases} 0, & \text{if } i < j, \\ \frac{1}{2}a_{ij}, & \text{if } i = j, \\ a_{ij}, & \text{if } i > j, \end{cases}$$

$$a_{ij}^2 = \begin{cases} a_{ij}, & \text{if } i < j, \\ \frac{1}{2}a_{ij}, & \text{if } i = j, \\ 0, & \text{if } i > j. \end{cases}$$

In fact, the discretized spatial problem operator (discretized matrix) is split into the lower and upper triangular matrices that are adjoint to each other. To solve the problem (3.6) using the above two-component splitting, we have the following factorized scheme written in a canonical form [19, 23, 24]:

$$(I + \sigma\tau\mathcal{A}_1)(I + \sigma\tau\mathcal{A}_2)\ \frac{P^{n+1} - P^n}{\tau} + \mathcal{A}P^n = \phi^n, \quad n = 0, 1, \cdots, N, \tag{3.12}$$

in which σ is a weight parameter and $\phi^n = f(\boldsymbol{x}, \sigma t^{n+1} + (1 - \sigma)t^n)$.

Taking $\sigma = 0.5$ corresponds to the classical Peaceman-Rachford scheme [16], while $\sigma = 1$ will result in Douglas-Rachford scheme [7]. Here, we take $\sigma = 1$ so (3.12) reduces to:

$$(I + \tau\mathcal{A}_1)(I + \tau\mathcal{A}_2)\ \frac{P^{n+1} - P^n}{\tau} + \mathcal{A}P^n = f^{n+1}, \quad n = 0, 1, \cdots, N. \tag{3.13}$$

The implementation of the ATM is based on the successive inversion of the operators $(I + \tau\mathcal{A}_1)$ and $(I + \tau\mathcal{A}_2)$. The scheme of ATM is unconditionally stable, but it has a restriction on a time step due to conditionally convergent since it has a term $\mathcal{O}(\tau^2 h^{-2})$ in the truncation error [24] and we will discuss it in section 5.2.

In the following, we propose two iterative modifications of the ATM scheme first by adding a correction term with the time derivative which is taken from the previous iteration level and second by introducing an iterative preconditioned method.

We first rewrite (3.13) as:

$$(I + \tau\mathcal{A}_1)(I + \tau\mathcal{A}_2)\ \delta P^{n+1} = f^{n+1} - \mathcal{A}P^n, \quad n = 0, 1, \cdots, N, \tag{3.14}$$

where

$$\delta P^{n+1} = \frac{P^{n+1} - P^n}{\tau}.$$

The modified ATM iterative scheme is presented by adding a correction term with the time derivative which is taken from the previous iteration level, reads as:

$$(I + \tau\mathcal{A}_1)(I + \tau\mathcal{A}_2)\ \delta P^{n+1,k+1} = f^{n+1} - \mathcal{A}P^n + \tau^2\mathcal{A}_1\ \mathcal{A}_2\ \delta P^{n+1,k}. \quad (3.15)$$

The other variation of ATM scheme is preconditioned iterative method. We design a preconditioned iterative method for equation (3.8) based on the two-component splitting introduced for the ATM scheme as follows:

$$\begin{aligned}(I + \tau\mathcal{A}_1)(I + \tau\mathcal{A}_2)(P^{n+1,k+1} - P^{n+1,k}) = (P^n + \tau f(P^{n+1,k}, S_w^n, S_o^n)) \\ - (I + \tau\mathcal{A})\ P^{n+1,k}.\end{aligned} \quad (3.16)$$

3.2 Coupling of Well and Flow Equation

Two types of well constraints need to be taken into account: either the well bottom hole pressure is given, i.e. the well is pressure-specified or a flow (production or injection) rate is given, i.e. the well is rate-specified. We assume that the minimum well bottom hole pressure is given for the producer and the rate is fixed for the injector. Therefore, for the producer the flow rates q_w and q_o are unknown and for the injector the well bottom hole pressure is unknown. The solution for either q_w and q_o or P_{bh} depends on the discretization technique for the flow equation (2.24). Different techniques for numerical solution of (2.24) are available, for instance, explicit, linearization, or fully implicit. Here

we focus on the linearization approach. The linearization of the well equations (2.28) and (2.29) results in the following equations:

$$q_w^{n+1} = WI\ \frac{k_{rw}^n}{\mu}\ P_c\ (P_{bh}^{n+1} - P^{n+1})\ \frac{1}{L_c^3}\ \delta(\boldsymbol{x} - \boldsymbol{x}^i), \tag{3.17}$$

$$q_o^{n+1} = WI\ \frac{k_{ro}^n}{\mu\beta}\ P_c\ (P_{bh}^{n+1} - P^{n+1})\ \frac{1}{L_c^3}\ \delta(\boldsymbol{x} - \boldsymbol{x}^i). \tag{3.18}$$

Equations (3.17) and (3.18) should be coupled to the flow equation (3.2) for the solution of the primary unknowns P and either P_{bh} or q_w and q_o.

For the injector, $q_w^{n+1} = q_{spec}$ is specified and $q_o^{n+1} = 0$ at i-th grid block. Thus, after substituting q_w^{n+1} to the right hand side of pressure equation (3.2) and solving for P^{n+1} we compute P_{bh}^{n+1} for the the injector well from (3.17).

For the producer, P_{bh}^{n+1} is specified at central location of the single perforation point at j-th grid block and q_w^{n+1}, and q_o^{n+1} are unknowns. We note that P_{bh}^{n+1} is the same for both phases. When $P \geq P_{bh}$ at j-th grid block, equations (3.17) and (3.18) need to be coupled to the flow equation (3.2). Also, as $P \geq P_{bh}$ oil and water will begin to produce (the production rates q_o and q_w are some negative values). Thus, after solving for P^{n+1} we calculate unknowns q_w^{n+1}, and q_o^{n+1}, from (3.17) and (3.18).

We represent f in (3.3) as:

$$f = f_g + f_r, \tag{3.19}$$

where

$$f_g(S_w, S_o) = \frac{\eta}{CP_c}\nabla.\Big((\Lambda_w + \beta^{-1}\alpha\Lambda_o)\nabla z\Big), \tag{3.20}$$

corresponds to the gravity term and,

$$f_r(P, S_w, S_o) = \frac{\zeta(1+\omega)}{CP_c}, \tag{3.21}$$

corresponds to sink/source flow rate.

In the injector grid, $q_w^{n+1} = q_{spec}$ and we have:

$$f_r = \frac{t_c}{CP_c}\ q_{spec}\ \delta(\boldsymbol{x} - \boldsymbol{x}^i),$$

and we represent it as:

$$f_r = \alpha_w\ \delta(\boldsymbol{x} - \boldsymbol{x}^i), \tag{3.22}$$

where

$$\alpha_w = \frac{t_c}{CP_c}\ q_{spec}.$$

In the producer grid, as $P \geq P_{bh}$ we substitute water and oil rates produced (3.17) and (3.18) into (3.21) at the location $\boldsymbol{x} = \boldsymbol{x}^j$ to get:

$$f_r = \frac{t_c}{CP_c}\ P_c\ \frac{1}{L_c^3} WI\Big(\frac{k_{rw}^n}{\mu} + \frac{k_{ro}^n}{\mu\beta}\Big)\ (P_{bh}^{n+1} - P^{n+1})\ \delta(\boldsymbol{x} - \boldsymbol{x}^j),$$

and this can be represented as:

$$f_r = \alpha_t\ (P_{bh}^{n+1} - P^{n+1})\ \delta(\boldsymbol{x} - \boldsymbol{x}^j), \tag{3.23}$$

where

$$\alpha_t = \frac{t_c}{CP_c}\ P_c\ \frac{1}{L_c^3} WI\Big(\frac{k_{rw}^n}{\mu} + \frac{k_{ro}^n}{\mu\beta}\Big).$$

We note that in the producer as $P < P_{bh}$ water and oil will not be produced i.e. $q_w = q_o = 0$. Thus, in this case we obtain:

$$f_r = 0. \tag{3.24}$$

Combining (3.19), (3.20), (3.22), and (3.23) into (3.8) for the case $P \geq P_{bh}$, we get:

$$\Big(I + \tau(A^n + \alpha_t^n W)\Big)P^{n+1} = P^n + \tau\Big(f_g^n + \alpha_t^n \ P_{bh}^{n+1} \ \delta(\boldsymbol{x} - \boldsymbol{x}^j) + \alpha_w \ \delta(\boldsymbol{x} - \boldsymbol{x}^i)\Big), \tag{3.25}$$

where W is a zero matrix with entry 1 on the diagonal at j-th row and j-th column corresponding to the producer well location.

$$W = \begin{array}{c} \\ \\ \\ \\ \\ \\ \\ \end{array} \begin{array}{c} \begin{array}{ccccccc} & & & j\text{-th} & & & \end{array} \\ \begin{pmatrix} 0 & 0 & \cdots & 0 & 0 & \cdots & 0 \\ \vdots & \vdots & \ddots & \ddots & \vdots & \vdots & \vdots \\ 0 & 0 & \cdots & 0 & 0 & \cdots & 0 \\ 0 & 0 & \cdots & 1 & 0 & \ddots & 0 \\ 0 & 0 & \cdots & 0 & 0 & \cdots & 0 \\ 0 & 0 & \cdots & 0 & 0 & 0 & 0 \end{pmatrix} \end{array} \begin{array}{l} \\ \\ \\ j\text{-th} \\ \\ \\ \end{array}$$

Combining (3.19), (3.20), (3.22), and (3.24) into (3.8) for the case $P < P_{bh}$, we get:

$$\Big(I + \tau A^n\Big)P^{n+1} = P^n + \tau\Big(f_g^n + \alpha_w \ \delta(\boldsymbol{x} - \boldsymbol{x}^i)\Big). \tag{3.26}$$

In the following subsections, we demonstrate the well equation coupling to the above splitting schemes for flow equation.

3.2.1 Well Coupling to the Summarized Scheme

The summarized scheme (3.10) for equation (3.25) with the well equation coupling for the case $P \geq P_{bh}$ reads as the following factorized form:

$$\begin{aligned} &\Big(I + \tau(A_1^n + \alpha_t^n W)\Big)\tilde{W}\Big(I + \tau(A_2^n + \alpha_t^n W)\Big)P^{n+1} \\ &= P^n + \tau\Big(f_g^n + \alpha_t^n\ P_{bh}^{n+1}\ \delta(\boldsymbol{x} - \boldsymbol{x}^j) + \alpha_w\ \delta(\boldsymbol{x} - \boldsymbol{x}^i)\Big), \end{aligned} \tag{3.27}$$

in which $\tilde{W} = (I + \tau\alpha_t W)^{-1}$. The splitting scheme corresponding to (3.27) solves the following set of two subproblems for the intermediate unknowns $P^{n+\alpha/2}$, $\alpha = 1, 2$, in 2D:

$$\begin{aligned} &\Big(I + \tau(A_1^n + \alpha_t^n W)\Big)P^{n+1/2} = P^n + \tau q^{n+1,1}, \\ &\Big(I + \tau(A_2^n + \alpha_t^n W)\Big)P^{n+1} = \tilde{W}^{-1}P^{n+1/2} + \tau q^{n+1,2}, \end{aligned} \tag{3.28}$$

Or equivalently:

$$\begin{aligned} &\frac{P^{n+1/2} - P^n}{\tau} + (A_1^n + \alpha_t^n W)P^{n+1/2} = q^{n+1,1}, \\ &\frac{P^{n+1} - P^{n+1/2}}{\tau} + (A_2^n + \alpha_t^n W)P^{n+1} = (\alpha_t^n W)P^{n+1/2} + q^{n+1,2}. \end{aligned} \tag{3.29}$$

Here, $f^{n+1} = q^{n+1,1} + q^{n+1,2}$ is an approximation to $f(\mathsf{P}(t^{n+1}), \mathsf{S}_w(t^n), \mathsf{S}_o(t^n))$. We also represent $q^{n+1,\alpha} = \bar{q}^{n+1,\alpha} + \tilde{q}^{n+1,\alpha}$, for $\alpha = 1, 2$, where $\sum_{\alpha=1}^{2} \bar{q}^{n+1,\alpha} = 0$. We need this representation to show the stability of the scheme in section 4.1. Similarly, the summarized scheme (3.10) for equation (3.26) with the well

equation coupling for the case $P < P_{bh}$ is:

$$\Big(I + \tau A_1^n\Big)\Big(I + \tau A_2^n\Big)P^{n+1} = P^n + \tau\Big(f_g^n + \alpha_w\ \delta(\boldsymbol{x} - \boldsymbol{x}^i)\Big), \tag{3.30}$$

and in the form of individual equations we have:

$$\begin{aligned} &\frac{P^{n+1/2} - P^n}{\tau} + A_1^n P^{n+1/2} = q^{n+1,1}, \\ &\frac{P^{n+1} - P^{n+1/2}}{\tau} + A_2^n P^{n+1} = q^{n+1,2}. \end{aligned} \tag{3.31}$$

The same representation for $q^{n+1,1}$, and $q^{n+1,2}$ is applied for this scheme as mentioned above. We separate the two cases in (3.29) and (3.31) as we discuss their stability differently.

The iterative preconditioned scheme (3.11) for equation (3.25) with the well equation coupling for the case $P \geq P_{bh}$ becomes:

$$\begin{aligned} &\Big(\tilde{W}^{-1} + \tau A_1^n\Big)\tilde{W}\Big(\tilde{W}^{-1} + \tau A_2^n\Big)\left(P^{n+1,k+1} - P^{n+1,k}\right) = \\ &\Big(P^n + \tau\Big(f_g^n + \alpha_t^n\ P_{bh}^{n+1}\ \delta(\boldsymbol{x} - \boldsymbol{x}^j) + \alpha_w\ \delta(\boldsymbol{x} - \boldsymbol{x}^i)\Big)\Big) \\ &\quad - \Big(I + \tau(A^n + \alpha_t^n W)\Big)P^{n+1,k}. \end{aligned} \tag{3.32}$$

For the case $P < P_{bh}$, the iterative preconditioned scheme (3.11) for equation (3.26) reads as:

$$\begin{aligned} &\Big(I + \tau A_1^n\Big)\Big(I + \tau A_2^n\Big)\left(P^{n+1,k+1} - P^{n+1,k}\right) = \\ &\Big(P^n + \tau\Big(f_g^n + \alpha_w\ \delta(\boldsymbol{x} - \boldsymbol{x}^i)\Big)\Big) - \Big(I + \tau A^n\Big)P^{n+1,k}. \end{aligned} \tag{3.33}$$

3.2.2 Well Coupling to the ATM Scheme

The ATM scheme (3.13) with the well equation coupling for the case $P \geq P_{bh}$ becomes:

$$\begin{aligned}
&\left(\tilde{W}^{-1} + \tau\mathcal{A}_1^n\right)\tilde{W}\left(\tilde{W}^{-1} + \tau\mathcal{A}_2^n\right)\,\delta P^{n+1} = \\
&\left(f_g^n + \alpha_t^n\;P_{bh}^{n+1}\;\delta(\boldsymbol{x}-\boldsymbol{x}^j) + \alpha_w\;\delta(\boldsymbol{x}-\boldsymbol{x}^i)\right) \\
&-\left(\mathcal{A}^n + \alpha_t^n W\right)P^n,
\end{aligned} \tag{3.34}$$

and for the case $P < P_{bh}$, it becomes:

$$\left(I + \tau\mathcal{A}_1^n\right)\left(I + \tau\mathcal{A}_2^n\right)\,\delta P^{n+1} = \left(f_g^n + \alpha_w\;\delta(\boldsymbol{x}-\boldsymbol{x}^i)\right) - \mathcal{A}^n P^n. \tag{3.35}$$

Modified ATM iterative scheme (3.15) with the well equation coupling for the case $P \geq P_{bh}$ has the following form:

$$\begin{aligned}
&\left(\tilde{W}^{-1} + \tau\mathcal{A}_1^n\right)\tilde{W}\left(\tilde{W}^{-1} + \tau\mathcal{A}_2^n\right)\,\delta P^{n+1,k+1} = \\
&\left(f_g^n + \alpha_t^n\;P_{bh}^{n+1}\;\delta(\boldsymbol{x}-\boldsymbol{x}^j) + \alpha_w\;\delta(\boldsymbol{x}-\boldsymbol{x}^i)\right) \\
&-\left(\mathcal{A}^n + \alpha_t^n W\right)P^n + \tau^2\mathcal{A}_1^n\;\tilde{W}\mathcal{A}_2^n\;\delta P^{n+1,k},
\end{aligned} \tag{3.36}$$

and for the case $P < P_{bh}$, it is:

$$\begin{aligned}
\left(I + \tau\mathcal{A}_1^n\right)\left(I + \tau\mathcal{A}_2^n\right)\,\delta P^{n+1,k+1} = &\left(f_g^n + \alpha_w\;\delta(\boldsymbol{x}-\boldsymbol{x}^i)\right) - \mathcal{A}^n P^n \\
&+ \tau^2\mathcal{A}_1^n\;\mathcal{A}_2^n\;\delta P^{n+1,k}.
\end{aligned} \tag{3.37}$$

The ATM preconditioned scheme (3.16) with coupling of the well equations is exactly the same scheme as the summarized preconditioned scheme with

coupled wells (3.32) and (3.33) with A_α to be replaced with discrete operators $\mathcal{A}_\alpha$, for $\alpha = 1, 2$, respectively. Thus, ATM preconditioned scheme (3.16) for the case $P \geq P_{bh}$ is:

$$\begin{aligned}
&\Big(\tilde{W}^{-1} + \tau\mathcal{A}_1^n\Big)\tilde{W}\Big(\tilde{W}^{-1} + \tau\mathcal{A}_2^n\Big)\left(P^{n+1,k+1} - P^{n+1,k}\right) = \\
&\qquad\Big(P^n + \tau\Big(f_g^n + \alpha_t^n\ P_{bh}^{n+1}\ \delta(\boldsymbol{x} - \boldsymbol{x}^j) + \alpha_w\ \delta(\boldsymbol{x} - \boldsymbol{x}^i)\Big)\Big) \\
&\qquad - \Big(I + \tau(\mathcal{A}^n + \alpha_t^n W)\Big)P^{n+1,k},
\end{aligned} \tag{3.38}$$

and for the case $P < P_{bh}$, the ATM preconditioned scheme (3.16) becomes:

$$\begin{aligned}
&\Big(I + \tau\mathcal{A}_1^n\Big)\Big(I + \tau\mathcal{A}_2^n\Big)\left(P^{n+1,k+1} - P^{n+1,k}\right) = \\
&\qquad\Big(P^n + \tau\Big(f_g^n + \alpha_w\ \delta(\boldsymbol{x} - \boldsymbol{x}^i)\Big)\Big) - \Big(I + \tau\mathcal{A}^n\Big)P^{n+1,k}.
\end{aligned} \tag{3.39}$$

3.3 Spatial Discretization

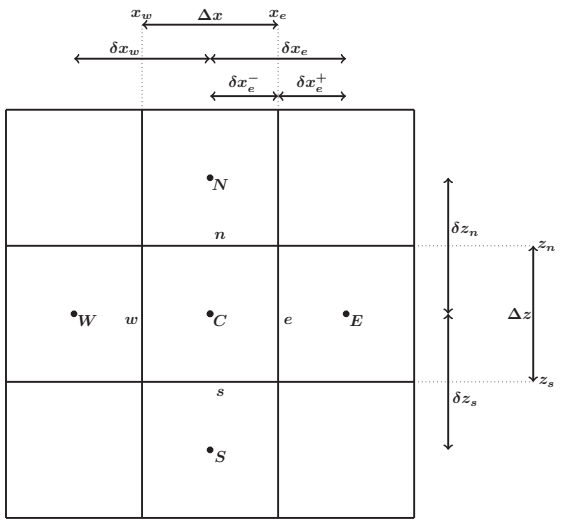

Figure 3.1: The MAC grid with geometric variables for a typical control-volume in 2D

For spatial discretization, in 2D, we assume that $\Omega = (0, L_1) \times (0, L_2)$ is partitioned into $N_1 N_2$ rectangles of size $\Delta x = L_1/N_1$, $\Delta z = L_2/N_2$. The cell centres of these subdomains have coordinates (x_C, z_C) with $x_C = (i - 1/2)\,\Delta x$, $z_C = (j - 1/2)\,\Delta z, i = 1, \ldots, N_1; j = 1, \ldots, N_2$. We denote Ω_{ij} to be the volume corresponding to a cell with centers at $(x_i, z_j), i = 1, \ldots, N_1; j = 1, \ldots, N_2$. An additional notation based on the direction on map is used to simplify the algebra. Figure 3.1 is a detailed sketch of one of the control volumes and its neighbours in the domain. The right and the left neighbours of C are called E for east and W for west and top and bottom neighbours of C are referred to as N and S for north and south, respectively. In general, the width of a control volume, Δx, will not be equal to the distance between C and its west and east neighbours, that is δx_w and δx_e. Also, the height of a control volume, Δz, will not be equal to the distance between C and its north and south neighbours, that is δz_n and δz_s. Regardless of the grid spacing, C is always located in the geometric centre of the its cell. Lower case subscripts refers to the location of the finite volume faces while upper case subscripts refers to the location of the nodes. The pressure and saturations are stored at the centroid of each cell. We integrate equations (3.7) and (3.5) over each Ω_{ij} cell and then apply the Gauss divergence theorem to simplify the terms containing second-order derivatives. We explain the spatial discretization for the flow equation (3.2) using a linearization approach. Spatial discretization for splitting scheme can be done in the same fashion as explain below. The only difference is that we have the spatial discretization only in one direction, x or z, depending on either A_1 or A_2 appears on each subproblem of the splitting

scheme.

$$
\begin{aligned}
\int_{\Omega_{ij}} \frac{P^{n+1}-P^n}{\tau}\, d\Omega &= \int_{z_s}^{z_n} \left(\left(\frac{\Lambda_t^n}{CP_c} \frac{\partial P^{n+1}}{\partial x} \right)_e - \left(\frac{\Lambda_t^n}{CP_c} \frac{\partial P^{n+1}}{\partial x} \right)_w \right) dz \\
&+ \int_{x_e}^{x_w} \left(\left(\frac{\Lambda_t^n}{CP_c} \frac{\partial P^{n+1}}{\partial z} \right)_n - \left(\frac{\Lambda_t^n}{CP_c} \frac{\partial P^{n+1}}{\partial z} \right)_s \right) dx + \int_{\Omega_{ij}} f^{n+1}\, d\Omega \\
&\approx \left(\left(\frac{\Lambda_t^n}{CP_c} \frac{\partial P^{n+1}}{\partial x} \right)_e - \left(\frac{\Lambda_t^n}{CP_c} \frac{\partial P^{n+1}}{\partial x} \right)_w \right) \Delta z \\
&+ \left(\left(\frac{\Lambda_t^n}{CP_c} \frac{\partial P^{n+1}}{\partial z} \right)_n - \left(\frac{\Lambda_t^n}{CP_c} \frac{\partial P^{n+1}}{\partial z} \right)_s \right) \Delta x + \int_{\Omega_{ij}} f^{n+1}\, d\Omega \qquad (3.40) \\
&\approx \frac{1}{CP_c} \left((\Lambda_t^n)_e \frac{P_E^{n+1}-P_C^{n+1}}{\delta x_e} - (\Lambda_t^n)_w \frac{P_C^{n+1}-P_W^{n+1}}{\delta x_w} \right) \Delta z \\
&+ \frac{1}{CP_c} \left((\Lambda_t^n)_n \frac{P_N^{n+1}-P_C^{n+1}}{\delta z_n} - (\Lambda_t^n)_s \frac{P_C^{n+1}-P_S^{n+1}}{\delta z_s} \right) \Delta x \\
&+ \int_{\Omega_{ij}} f^{n+1}\, d\Omega.
\end{aligned}
$$

The first term in the first row of (3.40) can be approximated by the mid-point quadrature rule as:

$$
\int_{\Omega_{ij}} \frac{P^{n+1}-P^n}{\tau}\, d\Omega \;\approx\; \Delta x \Delta z\, \frac{P_C^{n+1}-P_C^n}{\tau}.
$$

Also, we write the last term in the second row of (3.40) as:

$$
\int_{\Omega_{ij}} f^{n+1}\, d\Omega = \int_{\Omega_{ij}} f_g^n\, d\Omega + \int_{\Omega_{ij}} f_r^{n+1}\, d\Omega,
$$

and we approximate $\int_{\Omega_{ij}} f_g^n \, d\Omega$ applying the Gauss divergence theorem:

$$\begin{aligned}
\int_{\Omega_{ij}} f_g^n \, d\Omega &= \int_{\Omega_{ij}} \frac{\eta}{CP_c} \nabla \cdot \Big((\Lambda_w^n + \beta^{-1}\alpha\Lambda_o^n) \nabla z \Big) \, d\Omega \\
&\approx \frac{\eta}{CP_c} \left((\Lambda_w^n + \beta^{-1}\alpha\Lambda_o^n)_e \, \frac{z_E - z_C}{\delta x_e} - (\Lambda_w^n + \beta^{-1}\alpha\Lambda_o^n)_w \, \frac{z_C - z_W}{\delta x_w} \right) \Delta z \\
&+ \frac{\eta}{CP_c} \left((\Lambda_w^n + \beta^{-1}\alpha\Lambda_o^n)_n \, \frac{z_N - z_C}{\delta z_n} - (\Lambda_w^n + \beta^{-1}\alpha\Lambda_o^n)_s \, \frac{z_C - z_S}{\delta z_s} \right) \Delta x,
\end{aligned} \tag{3.41}$$

and approximating by the midpoint rule for $\int_{\Omega_{ij}} f_r^{n+1} \, d\Omega$ is:

$$\int_{\Omega_{ij}} f_r^{n+1} \, d\Omega \;\approx\; \Delta x \Delta z \; (f_r^{n+1})_C.$$

Equations (3.40) and (3.41) require the computation of $\Lambda_w, \Lambda_o, \Lambda_t, \alpha$, and β at the interfaces of the control volumes. They contain the rock property which is K, fluid property (density and viscosity) denoted as α and β and the rock/fluid property which is k_{rw} and k_{ro}. The weighted harmonic averaging, arithmetic averaging, and single-point upstream weighting are appropriate approximations, respectively. For example, for the value of K at the interface e, continuity at the interface requires,

$$K_C \, (\frac{\partial P}{\partial x})_{x_e^-} = K_E \, (\frac{\partial P}{\partial x})_{x_e^+} = K_e \, (\frac{\partial P}{\partial x})_{x_e}.$$

With central difference approximation to the above relation we get:

$$K_e = \frac{K_E K_C}{\gamma K_E + (1-\gamma) K_C},$$

where

$$\gamma = \frac{\delta x_{e^-}}{\delta x_e} = \frac{x_e - x_C}{x_E - x_C}.$$

For the case of equally distant grids, $\gamma = \frac{1}{2}$ and $K_e = \frac{2K_E K_C}{K_E + K_C}$. Similar formulation can be derived for K_w, K_n, and K_s.

From equation (2.25), the water phase potential difference at the interface n for instance is given by:

$$(\Delta\Phi_w)_n = (P_N - P_C) + \eta\ (z_N - z_C).$$

The upstream weighting value of k_{rw} at interface n is:

$$(k_{rw})_n = \begin{cases} (k_{rw})_N, & \text{if } (\Delta\Phi_w)_n > 0, \\ (k_{rw})_C, & \text{if } (\Delta\Phi_w)_n < 0. \end{cases}$$

When $(\Delta\Phi_w)_n > 0$, the flow of water is from block N to block C and as $(\Delta\Phi_w)_n < 0$, the flow of water is from block C to block N. For the oil phase and other interface similar formulation can be driven. We note that this approximation is only first order accurate.

It is easy to see that applying the above approximations to (3.40) leads to standard five-points stencil scheme for the pressure equation in 2D.

The space discretization for explicit scheme of (3.5) for the saturation

equation is as follows:

$$
\begin{aligned}
\int_{\Omega_{ij}} \phi \frac{S_w^{n+1} - S_w^n}{\tau}\, d\Omega &= \int_{z_s}^{z_n} \left(\left(\Lambda_w^n \frac{\partial P^{n+1}}{\partial x} \right)_e - \left(\Lambda_w^n \frac{\partial P^{n+1}}{\partial x} \right)_w \right) dz \\
&+ \int_{x_e}^{x_w} \left(\left(\Lambda_w^n \frac{\partial P^{n+1}}{\partial z} \right)_n - \left(\Lambda_w^n \frac{\partial P^{n+1}}{\partial z} \right)_s \right) dx \\
&+ \eta \int_{z_s}^{z_n} \left(\left(\Lambda_w^n \, \frac{\partial z}{\partial x} \right)_e - \left(\Lambda_w^n \, \frac{\partial z}{\partial x} \right)_w \right) dz \\
&+ \eta \int_{x_e}^{x_w} \left(\left(\Lambda_w^n \, \frac{\partial z}{\partial x} \right)_n - \left(\Lambda_w^n \, \frac{\partial z}{\partial x} \right)_s \right) dx \\
&+ \int_{\Omega_{ij}} \zeta^{n+1}\, d\Omega \\
&\approx \left((\Lambda_w^n)_e \, \frac{P_E^{n+1} - P_C^{n+1}}{\delta x_e} - (\Lambda_w^n)_w \, \frac{P_C^{n+1} - P_W^{n+1}}{\delta x_w} \right) \Delta z \\
&+ \left((\Lambda_w^n)_n \, \frac{P_N^{n+1} - P_C^{n+1}}{\delta z_n} - (\Lambda_w^n)_s \, \frac{P_C^{n+1} - P_S^{n+1}}{\delta z_s} \right) \Delta x \\
&+ \eta \left((\Lambda_w^n)_e \, \frac{z_E - z_C}{\delta x_e} - (\Lambda_w^n)_w \, \frac{z_C - z_W}{\delta x_w} \right) \Delta z \\
&+ \eta \left((\Lambda_w^n)_n \, \frac{z_N - z_C}{\delta z_n} - (\Lambda_w^n)_s \, \frac{z_C - z_S}{\delta z_s} \right) \Delta x \\
&+ \int_{\Omega_{ij}} \zeta^{n+1}\, d\Omega.
\end{aligned}
\tag{3.42}
$$

The first term in the first row of (3.42) can be approximated by the mid-point quadrature rule as:

$$
\int_{\Omega_{ij}} \phi \frac{S_w^{n+1} - S_w^n}{\tau}\, d\Omega \;\approx\; \Delta x \Delta z \, \frac{(S_w^{n+1} - S_w^n)_C}{\tau},
$$

and again we use the midpoint rule for $\int_{\Omega_{ij}} \zeta^{n+1}\, d\Omega$ to get:

$$\int_{\Omega_{ij}} \zeta_r^{n+1}\, d\Omega \;\approx\; \Delta x \Delta z\, (\zeta^{n+1})_C.$$

The explicit discretization (3.42) is only conditionally stable. That is, the time step must satisfy the following stability condition,

$$\tau \leq \min_{i,j} \left(\frac{1}{\frac{V_x}{\Delta x} + \frac{V_z}{\Delta z}} \right)_{i,j},$$

where the minimum is taken over all gridblocks. We denote velocity in x and z direction by V_x and V_z. They are derived from the water saturation equation (2.25) as follows:

$$V_x = \frac{K}{\phi} \frac{\partial k_{rw}}{\partial S_w} \frac{\partial P}{\partial x},$$

$$V_z = \frac{K}{\phi} \frac{\partial k_{rw}}{\partial S_w} \left(\frac{\partial P}{\partial z} + \eta \right).$$

We note that V_x and V_z are obtained by expanding the divergent operators in equation (2.25). Coefficients of $\frac{1}{\phi}\frac{\partial S_w}{\partial x}$ and $\frac{1}{\phi}\frac{\partial S_w}{\partial z}$ represent V_x and V_z respectively.

Chapter 4

Stability Analysis

In order to prove unconditional stability of the summarized scheme, the operators A_1 and A_2 should be positive semidefinite. First, we show the stability for the summarized scheme following the book of [23]. Next, the stability for the alternating triangle method will be discussed using [24].

4.1 Stability of the Summarized Scheme

Assume H is a Hilbert space with an inner product $(.,.)$ and $\| \, . \, \|$ is the norm generated in H by the inner product. Operators A, A_1, and A_2 as defined in 3.1.3 are linear, symmetric and positive semidefinite. We note that for the case $P < P_{bh}$ which is the scheme (3.31) we refer to the proof of stability which is theorem 5.2 of [23]. We write it in this thesis in theorem 4.1 without rewriting the detail of the proof. For the case $P \geq P_{bh}$ which is the scheme (3.28), the proof of stability is done by the author of this thesis by first proving lemma 4.1 similar to lemma 5.1 in the book [23] and then stability will be shown in theorem 4.2.

Theorem 4.1. *Assume that* $0.5 \leq \sigma_\alpha \leq 2$ *for* $\alpha = 1, \cdots, d$. *Then the solution to the following scheme*

$$\frac{P^{n+\alpha/d} - P^{n+(\alpha-1)/d}}{\tau} + A_\alpha(\sigma_\alpha P^{n+\alpha/d} + (1-\sigma_\alpha)P^{n+(\alpha-1)/d}) = q^{n+1,\alpha}$$

which solves the Cauchy problem (3.6) *of finding* $\mathsf{P}(t)$ *for* $t > 0$ *satisfies the a priori estimate for any* $\tau > 0$*:*

$$\left\|P^{n+1}\right\| \leq \|P^0\| + \sum_{k=0}^{n} \tau \sum_{\alpha=1}^{d} \left(\left\|\tilde{q}^{k,\alpha}\right\| + \tau \left\| A_\alpha \sum_{\beta=\alpha}^{d} \bar{q}^{k,\beta} \right\| \right),$$

where $f^{n+1} = \sum_{\alpha=1}^{d} q^{n+1,\alpha}$ *is some approximation to* $f(t^{n+1}, \boldsymbol{x})$. *With the representation of* $q^{n+1,\alpha} = \bar{q}^{n+1,\alpha} + \tilde{q}^{n+1,\alpha}$, *for* $\alpha = 1, 2, \cdots, d$, $\sum_{\alpha=1}^{d} \bar{q}^{n+1,\alpha} = 0$.

Proof. Since $(A_\alpha P, P) \geq 0$ for $P \in H$, and for $\alpha = 1, \cdots, d$, then by theorem 5.2 of [23] the estimate is immediate. □

Remark 4.1.1. *Theorem 4.1 also remains valid in the case of a variable operator* $A_\alpha = A_\alpha(t)$. *From the proof of the theorem this is obvious.*

Remark 4.1.2. *In our work* $d = 2$, *and we set* $\sigma_\alpha = 1$ *which results in the implicit scheme* (3.31) *for the case* $P < P_{bh}$.

To prove the stability for the scheme (3.28) for $P \geq P_{bh}$, we need the following lemma similar to lemma 5.1 in [23].

Lemma 4.1. *Let* $C = \tau(I + \tau(A_1 + \alpha_t W))^{-1}(A_1 + \alpha_t W)$, *where* I *is identity operator and* $(A_1 + \alpha_t W) \geq 0$. *Then, the following estimate holds:*

$$\|I - C\| \leq 1.$$

Proof. We have $\|I - C\| = \|I - C^*\|$, where C^* denotes the adjoint operator of C. Also, we have the following:

$$\|I - C\| \leq 1 \iff \|I - C^*\| \leq 1,$$

and,

$$\|I - C^*\|^2 = \|(I - C)(I - C^*)\|.$$

Therefore,

$$\begin{aligned} \|I - C^*\| \leq 1 &\iff \|(I - C)(I - C^*)\| \leq \|I\| \\ &\iff I - C^* - C + CC^* \leq I \\ &\iff CC^* \leq C + C^*. \end{aligned}$$

To show $\|I-C\| \leq 1$ we equivalently need to show $CC^* \leq C+C^*$. Substituting C and C^*, we get:

$$\tau(I + \tau(A_1 + \alpha_t W))^{-1}(A_1 + \alpha_t W)\ \tau\ (A_1 + \alpha_t W)^*(I + \tau(A_1^* + \alpha_t W^*))^{-1}$$

$$\leq \tau(I + \tau(A_1 + \alpha_t W))^{-1}(A_1 + \alpha_t W) + \tau\ (A_1 + \alpha_t W)^*(I + \tau(A_1^* + \alpha_t W^*))^{-1},$$

multiplying both side from the right by $(I + \tau(A_1^* + \alpha_t W^*))$, we get:

$$\tau(I + \tau(A_1 + \alpha_t W))^{-1}(A_1 + \alpha_t W)\ (A_1 + \alpha_t W)^*$$

$$\leq (I + \tau(A_1 + \alpha_t W))^{-1}(A_1 + \alpha_t W)(I + \tau(A_1^* + \alpha_t W^*)) + (A_1 + \alpha_t W)^*,$$

multiplying both side from the left by $(I + \tau(A_1 + \alpha_t W))$ yields:

$$\begin{aligned}
&\tau(A_1 + \alpha_t W)\ (A_1 + \alpha_t W)^* \\
&\leq (A_1 + \alpha_t W)\ (I + \tau(A_1^* + \alpha_t W^*)) + (I + \tau(A_1 + \alpha_t W))\ (A_1 + \alpha_t W)^* \\
&\leq (A_1 + \alpha_t W)\ \ + \tau(A_1 + \alpha_t W)(A_1 + \alpha_t W)^* + (A_1 + \alpha_t W)^* \\
&+ \tau(A_1 + \alpha_t W)(A_1 + \alpha_t W)^*.
\end{aligned}$$

Therefore, we get:

$$\begin{aligned}
&\tau(A_1 + \alpha_t W)(A_1 + \alpha_t W)^* + (A_1 + \alpha_t W) + (A_1 + \alpha_t W)^* \geq 0 \\
&\iff (A_1 + \alpha_t W) \geq 0,\ (A_1 + \alpha_t W)^* \geq 0.
\end{aligned}$$

From the assumption of the lemma, $(A_1 + \alpha_t W) \geq 0$, and $(A_1 + \alpha_t W)^* \geq 0$ are satisfied, therefore $CC^* \leq C + C^*$, and then equivalently $\|I - C^*\| \leq 1$. $\square$

We rewrite each subproblem (3.28) as:

$$\begin{aligned}
P^{n+1/2} &= \left((\tilde{W}^{-1})^n + \tau A_1^n\right)^{-1} P^n + \tau \left((\tilde{W}^{-1})^n + \tau A_1^n\right)^{-1} q^{n+1,1}, \\
P^{n+1} &= \left((\tilde{W}^{-1})^n + \tau A_2^n\right)^{-1} \left(\tilde{W}^{-1}\right)^n P^{n+1/2} + \tau \left((\tilde{W}^{-1})^n + \tau A_2^n\right)^{-1} q^{n+1,2}.
\end{aligned} \tag{4.1}$$

From the definition $(\tilde{W}^{-1} + \tau A_1)^{-1} = (I + \tau(A_1 + \alpha_t W))^{-1}$. Since

$$(I + \tau(A_1 + \alpha_t W)) - \tau(A_1 + \alpha_t W) = I,$$

we multiply $(I+\tau(A_1+\alpha_t W))^{-1}$ from the left to get:

$$I-\tau\ (I+\tau(A_1+\alpha_t W))^{-1}(A_1+\alpha_t W)=(I+\tau(A_1+\alpha_t W))^{-1}.$$

We call $C=\tau(I+\tau(A_1+\alpha_t W))^{-1}(A_1+\alpha_t W)$, because $A_1\geq 0$, and $\alpha_t\geq 0$ then $(A_1+\alpha_t W)\geq 0$. It follows from Lemma 4.1 $\|I-C\|\leq 1$ which results in $\|(I+\tau(A_1+\alpha_t W))^{-1}\|\leq 1$. A similar approach can be taken to show that $\|(I+\tau(A_2+\alpha_t W))^{-1}\|\leq 1$.

Taking the norm of the first subproblem in (4.1) and using lemma 4.1, we get:

$$\begin{aligned}\left\|P^{n+1/2}\right\| &\leq \left\|\left((\tilde{W}^{-1})^n+\tau A_1^n\right)^{-1}\right\|\ \|P^n\|+\tau\ \left\|\left((\tilde{W}^{-1})^n+\tau A_1^n\right)^{-1}\right\|\ \left\|q^{n+1,1}\right\|,\\ &\leq \|P^n\|+\tau\ \left\|q^{n+1,1}\right\|.\end{aligned}\tag{4.2}$$

Taking the norm of the second subproblem in (4.1) and using lemma 4.1, it yields:

$$\begin{aligned}\left\|P^{n+1}\right\| &\leq \left\|\left((\tilde{W}^{-1})^n+\tau A_2^n\right)^{-1}\right\|\ \left\|\left(\tilde{W}^{-1}\right)^n\right\|\ \left\|P^{n+1/2}\right\|\\ &\quad+\tau\ \left\|\left((\tilde{W}^{-1})^n+\tau A_2^n\right)^{-1}\right\|\ \left\|q^{n+1,2}\right\|\\ &\leq \left\|(\tilde{W}^{-1})^n\right\|\ \left\|P^{n+1/2}\right\|+\tau\ \left\|q^{n+1,2}\right\|.\end{aligned}\tag{4.3}$$

Substituting (4.2) into (4.3), yields the inequality:

$$\left\|P^{n+1}\right\|\leq \left\|(\tilde{W}^{-1})^n\right\|\ \left(\|P^n\|+\tau\ \left\|q^{n+1,1}\right\|\right)+\tau\ \left\|q^{n+1,2}\right\|.\tag{4.4}$$

The inequality (4.4) implies the desired estimate for stability with respect to the initial data and the right hand side. We summarize the result in the following theorem.

Theorem 4.2. *The proposed scheme* (3.28) *is unconditionally stable and we have the following estimate:*

$$\begin{aligned}\left\|P^{N+1}\right\| \leq & \prod_{k=0}^{N}\left\|(\tilde{W}^{-1})^{k}\right\|\left\|P^{0}\right\| \\ & + \tau\sum_{k=1}^{N+1}\left(\prod_{l=1}^{N-k+2}\left\|(\tilde{W}^{-1})^{l}\right\|\left\|q^{k,1}\right\| + \prod_{l=1}^{N-k+1}\left\|(\tilde{W}^{-1})^{l}\right\|\left\|q^{k,2}\right\|\right).\end{aligned}$$

4.2 Stability of the ATM Scheme

We show unconditional stability of the ATM scheme following the idea of [24]. The proof demonstrated there is in H_A, but we prove the unconditionally stability in different space H_{C_s} due to semidefiniteness of $\mathcal{A}$ in our problem.

Theorem 4.3. *The alternating triangle method* (3.12) *is unconditionally stable under the restriction* $\sigma \geq 0.5$ *and the following a priori estimate holds:*

$$\sum_{k=0}^{N-1}\tau\left\|\frac{P^{k+1}-P^{k}}{\tau}\right\|_{C_s}^{2} + |P^{N}|_{\mathcal{A}}^{2} \leq |P^{0}|_{\mathcal{A}}^{2} + \sum_{k=0}^{N-1}\tau\left\|\phi^{k}\right\|_{C_s{}^{-1}}^{2}$$

Proof. The factorized operator,

$$B = (I+\sigma\tau\mathcal{A}_1)(I+\sigma\tau\mathcal{A}_2),$$

is self-adjoint and positive definite for $\sigma \geq 0$. That is,

$$B = B^* = I + \sigma\tau\mathcal{A} + \sigma^2\tau^2\mathcal{A}_1\mathcal{A}_2 \geq I + \sigma\tau\mathcal{A},$$

and for $\sigma \geq 0.5$,

$$B - \frac{\tau}{2}\mathcal{A} \geq I > 0.$$

We denote $C = B - \frac{\tau}{2}\mathcal{A}$. The operator C may be represented as the sum of a self-adjoint operator and a skew-symmetric operator:

$$C = C_s + C_a,$$

where

$$C_s = \frac{1}{2}(C + C^*), \qquad C_a = \frac{1}{2}(C - C^*).$$

We can write scheme (3.12) in an equivalent form:

$$C\ \frac{P^{n+1} - P^n}{\tau} + \mathcal{A}\frac{P^{n+1} + P^n}{2} = \phi^n. \tag{4.5}$$

Taking inner product of (4.5) by $2\left(\frac{P^{n+1} - P^n}{\tau}\right)$ yields:

$$\begin{aligned} &2\left(C_s\ \frac{P^{n+1} - P^n}{\tau}, \frac{P^{n+1} - P^n}{\tau}\right) + \frac{1}{\tau}(\mathcal{A}P^{n+1}, P^{n+1}) - \frac{1}{\tau}(\mathcal{A}P^n, P^n), \\ &= 2\left(\phi^n, \frac{P^{n+1} - P^n}{\tau}\right). \end{aligned} \tag{4.6}$$

We note that $C_a^* = -C_a$, and $(C_a v, v) = 0$ for all $v \in H$. Then (4.6) can be

written as:

$$2\left\|\frac{P^{n+1}-P^n}{\tau}\right\|_{C_s}^2+\frac{1}{\tau}\,|P^{n+1}|_{\mathcal{A}}^2=\frac{1}{\tau}\,|P^n|_{\mathcal{A}}^2+2\left(\phi^n,\frac{P^{n+1}-P^n}{\tau}\right),\tag{4.7}$$

where $|.|_{\mathcal{A}}$ denote seminorm generated by $\mathcal{A}$. For the last term in (4.7) using Cauchy-Schwarz inequality and then Young's inequality we have:

$$\begin{aligned}\left(\phi^n,\frac{P^{n+1}-P^n}{\tau}\right)&\leq\ \|\phi^n\|_{{C_s}^{-1}}\left\|\frac{P^{n+1}-P^n}{\tau}\right\|_{C_s}\\&\leq\frac{\|\phi^n\|_{{C_s}^{-1}}^2}{2}+\frac{\left\|\frac{P^{n+1}-P^n}{\tau}\right\|_{C_s}^2}{2}.\end{aligned}$$

Substituting the above inequality into (4.7) yields:

$$\left\|\frac{P^{n+1}-P^n}{\tau}\right\|_{C_s}^2+\frac{1}{\tau}\,|P^{n+1}|_{\mathcal{A}}^2\leq\ \frac{1}{\tau}\,|P^n|_{\mathcal{A}}^2+\|\phi^n\|_{{C_s}^{-1}}^2.\tag{4.8}$$

The summation over all k from 0 to $N-1$ and multiplying (4.8) by τ yields the desired estimate for stability with respect to initial data and the right-hand side,

$$\sum_{k=0}^{N-1}\tau\left\|\frac{P^{k+1}-P^k}{\tau}\right\|_{C_s}^2+|P^N|_{\mathcal{A}}^2\leq\ |P^0|_{\mathcal{A}}^2+\sum_{k=0}^{N-1}\tau\left\|\phi^k\right\|_{{C_s}^{-1}}^2.$$

□

Remark 4.3.1. *Theorem 4.3 remains valid also in the case of a variable operator $B=B(t)$.*

Remark 4.3.2. *Theorem 4.3 with wells coupling for case $P\geq P_{bh}$ for scheme (3.34) is still valid. The only difference is with $\sigma=1$, $B=I+\tau\mathcal{A}+\tau^2\mathcal{A}_1\mathcal{A}_2+\tau\alpha_t W$ and still $C=B-\frac{\tau}{2}\mathcal{A}>0$ is true.*

Chapter 5

Convergence Analysis

We first investigate the convergence analysis for the summarized scheme. The convergence analysis is done in the framework of the book [23]. The convergence analysis for the alternating triangle method follows afterwards following the work of [24].

5.1 Summarized Scheme

5.1.1 Truncation Error in Time

Let $e = P - \mathsf{P}$, be the error between the discrete solution, P, and the exact solution P. Let $e^{n+\alpha/2} = P^{n+\alpha/2} - \mathsf{P}^{n+\alpha/2}, \alpha = 1, 2$. Now using this relation, we substitute P into the scheme (3.31) to get the error equation as the following:

$$\begin{aligned} \frac{e^{n+1/2} - e^n}{\tau} + A_1\, e^{n+1/2} &= -\frac{\mathsf{P}^{n+1/2} - \mathsf{P}^n}{\tau} - A_1\, \mathsf{P}^{n+1/2} + q^{n+1,1}, \\ \frac{e^{n+1} - e^{n+1/2}}{\tau} + A_2\, e^{n+1} &= -\frac{\mathsf{P}^{n+1} - \mathsf{P}^{n+1/2}}{\tau} - A_2\, \mathsf{P}^{n+1} + q^{n+1,2}. \end{aligned} \tag{5.1}$$

The truncation error of the individual equations is as follows:

$$\begin{aligned}\psi^{n+1,1} &= -\frac{\mathsf{P}^{n+1/2}-\mathsf{P}^{n}}{\tau} - A_1\ \mathsf{P}^{n+1/2} + q^{n+1,1},\\ \psi^{n+1,2} &= -\frac{\mathsf{P}^{n+1}-\mathsf{P}^{n+1/2}}{\tau} - A_2\ \mathsf{P}^{n+1} + q^{n+1,2}.\end{aligned} \tag{5.2}$$

For the truncation error, we have the following form [23]:

$$\psi^{n+1,\alpha} = \bar{\psi}^{n+1,\alpha} + \tilde{\psi}^{n+1,\alpha}, \alpha = 1,2, \qquad \bar{\psi}^{n+1,1} + \bar{\psi}^{n+1,2} = 0. \tag{5.3}$$

Also, we let,

$$\bar{\psi}^{n+1,\alpha} = -\frac{1}{2}\frac{\partial \mathsf{P}}{\partial t} - A_\alpha \mathsf{P}(t) + f_\alpha, \quad \alpha = 1,2, \qquad f_1 + f_2 = f. \tag{5.4}$$

From (5.2)-(5.4), and due to Taylor's expansion of P, we obtain an estimate for $\tilde{\psi}^{n+1,\alpha}$:

$$\begin{aligned}\tilde{\psi}^{n+1,1} &= \psi^{n+1,1} - \bar{\psi}^{n+1,1}\\ &= \left[-\frac{\mathsf{P}^{n+1/2}-\mathsf{P}^{n}}{\tau} - A_1\ \mathsf{P}^{n+1/2} + q^{n+1,1}\right]\\ &- \left[-\frac{1}{2}\frac{\partial \mathsf{P}}{\partial t} - A_1\mathsf{P}(t) + f_1\right]^{t^{n+1/2}}\\ &= \mathcal{O}(\tau),\end{aligned} \tag{5.5}$$

and similarly for the second subproblem,

$$\begin{aligned}
\tilde{\psi}^{n+1,2} &= \psi^{n+1,2} - \bar{\psi}^{n+1,2} \\
&= \left[-\frac{\mathsf{P}^{n+1} - \mathsf{P}^{n+1/2}}{\tau} - A_2\ \mathsf{P}^{n+1} + q^{n+1,2} \right] \\
&- \left[-\frac{1}{2}\frac{\partial \mathsf{P}}{\partial t} - A_2 \mathsf{P}(t) + f_2 \right]^{t^{n+1}} \\
&= \mathcal{O}(\tau).
\end{aligned} \tag{5.6}$$

Therefore, the truncation error in time for $n = 0, 1, \cdots$ is of $\mathcal{O}(\tau)$.

5.1.2 Error Estimate

We recall from (5.1) that the error satisfies:

$$\begin{aligned}
\frac{e^{n+1/2} - e^{n}}{\tau} + A_1\ e^{n+1/2} &= \psi^{n+1,1}, \\
\frac{e^{n+1} - e^{n+1/2}}{\tau} + A_2\ e^{n+1} &= \psi^{n+1,2},
\end{aligned} \tag{5.7}$$

which is the scheme (3.31) with different right hand side. By applying theorem 4.1, the error of the approximated solution satisfies:

$$\left\| e^{n+1} \right\| \leq \left\| e^{0} \right\| + \sum_{k=0}^{n} \tau \sum_{\alpha=1}^{2} \left(\left\| \tilde{\psi}^{k,\alpha} \right\| + \tau \left\| A_\alpha \sum_{\beta=\alpha}^{2} \bar{\psi}^{k,\beta} \right\| \right).$$

Since $e^0 = 0$, and using (5.3)-(5.6) we get the error estimate in time as:

$$\tau \sum_{k=0}^{n} \sum_{\alpha=1}^{2} \left(\left\| \tilde{\psi}^{k,\alpha} \right\| + \tau \left\| A_\alpha \sum_{\beta=\alpha}^{2} \bar{\psi}^{k,\beta} \right\| \right) = \mathcal{O}(\tau).$$

The result is summarized in the following theorem:

Theorem 5.1. *The proposed scheme* (3.31) *is convergent in time with convergent rate* $\mathcal{O}(\tau)$*, that is:*

$$\left\|e^{n+1}\right\| \leq \sum_{k=0}^{n} \tau \sum_{\alpha=1}^{2} \left(\left\|\tilde{\psi}^{k,\alpha}\right\| + \tau \left\| A_\alpha \sum_{\beta=\alpha}^{2} \bar{\psi}^{k,\beta} \right\| \right).$$

5.2 ATM Scheme

5.2.1 Truncation Error Estimate

By substituting P into the scheme (3.12) and using $e = P - \mathsf{P}$, we can get the error equation as follows:

$$B\ \frac{e^{n+1} - e^n}{\tau} + \mathcal{A}\ e^n = \psi^n, \tag{5.8}$$

where $B = (I + \sigma\tau\mathcal{A}_1)(I + \sigma\tau\mathcal{A}_2)$ and ψ^n is the truncation error that has the following form:

$$\psi^n = \phi^n - B\ \frac{\mathsf{P}^{n+1} - \mathsf{P}^n}{\tau} - \mathcal{A}\ \mathsf{P}^n, \tag{5.9}$$

in which $\phi^n = f(\boldsymbol{x}, t^{n+1})$ and f satisfies the problem (3.6). From theorem 2 of [24], the truncation error can be written as the following form:

$$\psi^n = \psi^n_\sigma + \psi^n_s, \tag{5.10}$$

where

$$\begin{aligned} \psi^n_\sigma &= (\sigma - \frac{1}{2})\ \tau\ \frac{d^2\mathsf{P}}{dt^2}(t^{n+1/2}) + \mathcal{O}(\tau^2), \\ \psi^n_s &= -\sigma^2\ \tau^2\ \mathcal{A}_1\mathcal{A}_2\ \frac{d\mathsf{P}}{dt}(t^{n+1/2}) + \mathcal{O}(\tau^3). \end{aligned} \tag{5.11}$$

For the first part of the truncation error, we have $\psi_\sigma^n = \mathcal{O}(\tau^2)$ for $\sigma = 0.5$, and $\psi_\sigma^n = \mathcal{O}(\tau)$ for $\sigma \neq 0.5$. For the second part of the truncation error, taking into account the explicit representation for operators $\mathcal{A}_1$ and $\mathcal{A}_2$, we have $\psi_s^n = \mathcal{O}(\tau^2|h|^{-2})$.

5.2.2 Error Estimate

Application of theorem 4.3 to equation (5.8) results in:

$$\sum_{k=0}^{N-1} \tau \left\| \frac{e^{k+1} - e^k}{\tau} \right\|_{C_s}^2 + |e^N|_{\mathcal{A}}^2 \leq \ |e^0|_{\mathcal{A}}^2 + \sum_{k=0}^{N-1} \tau \left\| \psi^k \right\|_{C_s{}^{-1}}^2.$$

Since $e^0 = 0$, and using (5.10), and (5.11), we get:

$$\begin{aligned} \sum_{k=0}^{N-1} \tau \left\| \frac{e^{k+1} - e^k}{\tau} \right\|_{C_s}^2 + |e^N|_{\mathcal{A}}^2 \leq \ & \sum_{k=0}^{N-1} \tau \left\| \psi^k \right\|_{C_s{}^{-1}}^2 \\ & \leq M \left(\left(\sigma - \frac{1}{2} \right) \tau + \tau^2 |h|^{-2} \right)^2, \end{aligned}$$

for some $M > 0$. This shows the conditionally convergent of the scheme (3.12).

Chapter 6

Numerical Results

In these experiments, we use the first model data from the 10th SPE Comparative Solution Project [3] for two-phase (water-oil) model. The domain is $762\times7.62\times15.24\ m^3$ with $100\times1\times2$ cells. The bottom of the model is at the origin with an initial pressure of 895 kPa at the first row of the discretized grid blocks. Initially, we set $S_w = 0.6$ and $S_o = 0.4$. The relative permeabilities are shown in table 6.1 and in figure 6.1. There is one injector in the top right corner at cell (100, 1, 2) and one producer in the bottom left corner at cell (1, 1, 1). The injection rate is set to be 200 kg/day and the producer is set to produce at a constant bottom hole pressure (P_{bh}) 1345 kPa. Both wells have a wellbore radius $r_w = 0.04\ m$ with $CC = 0.247$, $f = 1$ and $S = 0$. The initial properties are as follows: $K = 5.9215398 \times 10^{-6}\mu m^2$, $\phi = 0.32$, $\mu_w = 0.00116\ kg/(m.s)$, $\mu_o = 0.1211\ kg/(m.s)$, $\rho_w = 1001\ kg/m^3$, $\rho_o = 1015\ kg/m^3$ and $C = 4.8\times10^{-6}\ kPa^{-1}$. We run the simulation until $T = 5000$ days. With nondimensionalization, we have $K = 1$, $\Delta x = \Delta y = \Delta z = 0.01$, $\Omega = [0, 1] \times [0, 0.01] \times [0, 0.02]$ and $t \in [0, 5]$.

We solve the problem using linearized scheme for the pressure and an ex-

plicit scheme for the saturation (3.40) and (3.42) respectively. These solutions are considered as reference solutions and we call them non-spilt solutions. The splitting approximate solutions for pressure will be compared to the reference solution.

In the following sections, $\bar{P}$ and $\bar{S}_w$ denote the non-split solutions and P and S_w denote the split solutions.

Let $e^j \in \mathbb{R}^n$ be the error at the j-th time level. We define the norm $\|.\|_{l^2(\Omega)}$ as follows:

$$\left\|e^j\right\|_{l^2(\Omega)} = \left(\sum_{i=1}^{n} h_x h_z \ |e_i^j|^2\right)^{\frac{1}{2}},$$

where h_x and h_z are the grid size in x and z direction, respectively.

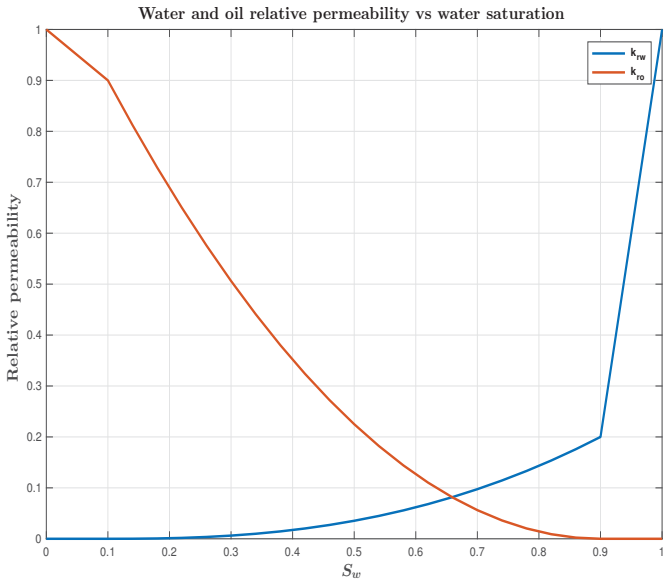

Figure 6.1: Relative permeabilities for water and oil

Table 6.1: Relative permeability

S_w	k_{rw}	k_{ro}
0.000000	0.000000	1.000000
0.033333	0.000000	0.966667
0.066667	0.000000	0.933333
0.100000	0.000000	0.900000
0.140000	0.000112	0.812250
0.180000	0.000632	0.729000
0.220000	0.001743	0.650250
0.260000	0.003578	0.576000
0.300000	0.006250	0.506250
0.340000	0.009859	0.441000
0.380000	0.014494	0.380250
0.420000	0.020239	0.324000
0.460000	0.027168	0.272250
0.500000	0.035355	0.225000
0.540000	0.044868	0.182250
0.580000	0.055771	0.144000
0.620000	0.068126	0.110250
0.660000	0.081993	0.081000
0.700000	0.097428	0.056250
0.740000	0.114487	0.036000
0.780000	0.133222	0.020250
0.820000	0.153687	0.009000
0.860000	0.175930	0.002250
0.900000	0.200000	0.000000
0.933333	0.466667	0.000000
0.966667	0.733333	0.000000
1.000000	1.000000	0.000000

6.1 Summarized Preconditioned Scheme

We solve the pressure equation using the preconditioned schemes (3.32)-(3.33) and couple the saturation equation using scheme (3.42) applying the algorithm 1:

while *TimeStep* $<$ *Final TimeStep* **do**

  Initialize $k := 0$; $P^{n+1,0} := P^n$;

  while $\left\| \frac{P^{n+1,k+1} - P^{n+1,k}}{P^{n+1,k}} \right\|_\infty > Tol_P$ **do**

    if $P < P_{bh}$ **then**

      Solve for $P^{n+1,k+1}$ using (3.33);

    else

      Solve for $P^{n+1,k+1}$ using (3.32);

    end

  end

  For some K, set $P^{n+1} := P^{n+1,K}$;

  Solve for S_w using (3.42);

end

Algorithm 1: Summarized preconditioned scheme

To study the temporal convergence without grid refinement, we define [13]:

$$\mathrm{TCR}(P, \tau) = \log_2 \left(\frac{\left\| P^\tau - P^{\frac{\tau}{2}} \right\|_2}{\left\| P^{\frac{\tau}{2}} - P^{\frac{\tau}{4}} \right\|_2} \right),$$

where P^τ denotes the pressure obtained using a time step τ. Because of the form of TCR, the spatial discretization error cancels and if the leading order temporal truncation error in the scheme is of $\mathcal{O}(\tau^p)$ then for small τ, TCR will equal p.

To show TCR for our numerical results, we run our program for the schemes (3.32)-(3.33) using the algorithm 1, with Tol_P =1e-7, final time $T = 5$ and different time steps τ. The reference solution was obtained with τ = 3.125e-

5. The results are shown on the table 6.2. We can see better than first order convergence for the pressure and the water saturation. In fact, the results show better order of convergence in practice than the theory given in the section 5.1 for the pressure.

Table 6.2: Temporal convergence of the l^2 norm of the error in the solution of the schemes (3.32)-(3.33) as compared to the reference solution normalized by the norm of the reference solution for the pressure at the final time $T = 5$.

τ	$\left\|\bar{P} - P\right\|_2 / \left\|\bar{P}\right\|_2$	TCR	$\left\|\bar{S_w} - S_w\right\|_2$	TCR
1e-3	6.0539e-7	2	9.2840e-5	1.89
5e-4	1.8006e-7	1.26	2.6444e-5	1.70
2.5e-4	7.4389e-8	1.33	8.5543e-6	1.27
1.25e-4	2.6855e-8	1.24	3.0628e-6	1.93
6.25e-5	8.1019e-9	–	7.9294e-7	–
3.125e-5	1.4647e-9	–	1.9897e-7	–

6.2 Alternating Triangle Scheme

We implement the modified ATM iterative schemes (3.36)-(3.37) applying the algorithm 2:

while *TimeStep* $<$ *Final TimeStep* **do**

  Initialize $k := 0; \delta P^{n+1,0} := 0;$

  while $\left\|\delta P^{n+1,k+1} - \delta P^{n+1,k}\right\| > Tol_\delta$ **do**

    if $P < P_{bh}$ **then**

      Solve for $P^{n+1,k+1}$ using (3.37);

    else

      Solve for $P^{n+1,k+1}$ using (3.36);

    end

  end

  For some K, set $P^{n+1} := P^n + \tau\ \delta P^{n+1,K}$;

  Solve for S_w using (3.42);

end

Algorithm 2: Modified ATM iterative scheme

We present temporal convergence for the schemes (3.36)-(3.37) applying the algorithm 2 with tolerance Tol_δ =1e-4 at the final time $T = 5$ in the table 6.3. It shows the second order convergence for the pressure and better than order one for the water saturation.

We also present temporal convergence for the ATM preconditioned schemes (3.38)-(3.39) applying the algorithm 1 with the pressure tolerance Tol_P =1e-7 at the final time $T = 5$ as shown on the table 6.4. We can see better than order one convergence for the pressure and the water saturation.

As we see, the summarized preconditioned scheme gives more accurate results compare to the modified ATM iterative scheme and ATM preconditioned scheme. The temporal convergence of the pressure for the summarized

Table 6.3: Temporal convergence of the l^2 norm of the error in the solution of the schemes (3.36)-(3.37) as compared to the reference solution normalized by the norm of the reference solution for the pressure at the final time $T = 5$.

τ	$\left\|\bar{P} - P\right\|_2 / \left\|\bar{P}\right\|_2$	TCR	$\left\|\bar{S_w} - S_w\right\|_2$	TCR
1e-3	4.4469e-3	2.92	2.9862e-3	2.37
5e-4	3.7743e-4	2.23	5.4237e-4	2.74
2.5e-4	1.5929e-4	1.73	9.4980e-5	1.99
1.25e-4	4.5242e-5	2.00	2.5589e-5	1.86
6.25e-5	1.0863e-5	–	6.9164e-6	–
3.125e-5	2.3202e-6	–	1.7692e-6	–

Table 6.4: Temporal convergence of the l^2 norm of the error in the solution of the schemes (3.38)-(3.39) as compared to the reference solution normalized by the norm of the reference solution for the pressure at the final time $T = 5$.

τ	$\left\|\bar{P} - P\right\|_2 / \left\|\bar{P}\right\|_2$	TCR	$\left\|\bar{S_w} - S_w\right\|_2$	TCR
1e-3	4.2728e-3	0.62	2.7035e-3	1.03
5e-4	1.5733e-3	2.83	1.1511e-3	1.34
2.5e-4	1.8316e-4	1.12	3.6428e-4	2.33
1.25e-4	6.4429e-5	1.55	8.6785e-5	1.69
6.25e-5	4.9374e-5	–	2.7451e-5	–
3.125e-5	1.0856e-5	–	9.8235e-6	–

preconditioned scheme is approximately 1.2 order and for the modified ATM iterative scheme is approximately 2 order and for ATM preconditioned scheme is approximately 1.5 order.

In order to improve the convergence of the ATM scheme, we added a correction term $\tau^2 \mathcal{A}_1 \mathcal{A}_2 \delta P^{n+1,k}$ to the right hand side of the scheme (3.15) and we got the modified ATM iterative schemes (3.36)-(3.37). The numerical results of the schemes (3.36)-(3.37) show that the order of convergence is increased

by one.

Due to the conditional consistency of the schemes (3.36)-(3.39), we cannot choose $\tau = \mathcal{O}(\Delta x)$, so we run simulations using $\tau =$ 1e-3. On the other hand, for the summarized preconditioned scheme, there is no restriction on the time step.

The time history of the numerical results for the pressure in the production and the injection well are compared in figure 6.2. The figure shows that the summarized preconditioned scheme matches with the non-split scheme while the other two ATM methods, modified ATM iterative scheme and ATM preconditioned, have delay to reach the minimum bottom hole pressure. We also compare the time history of the numerical results for the water saturation in the production and the injection well in figure 6.3. It shows that the summarized preconditioned scheme matches with the non-split scheme while the other two ATM schemes have some deviation. The time history of the numerical results for oil and water produced are presented on figure 6.4. As a consequence of the pressure delay mentioned above on figure 6.2, we expect to have some delay for the production well to be open for the two ATM schemes. Also, due to deviation of the water and oil saturation for the ATM schemes compared to the reference solution, they all cause different amount of oil and water to be produced using the ATM schemes and figure 6.4 confirms this. On the other hand, figure 6.4 shows that the summarized preconditioned scheme is in good agreement with the reference solution.

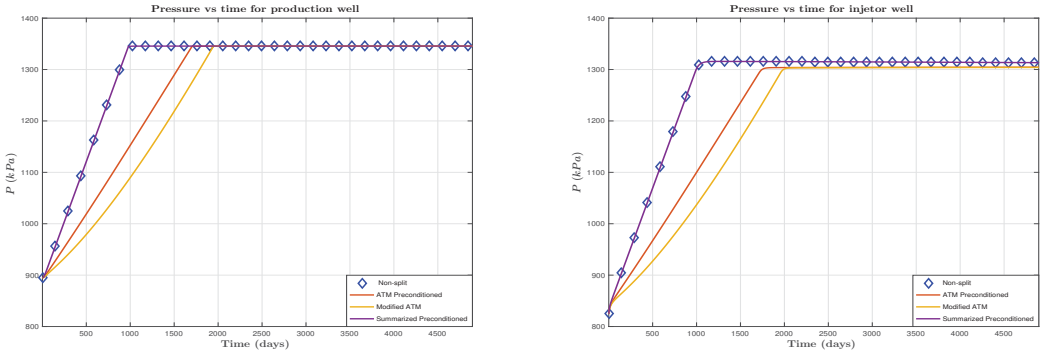

Figure 6.2: Comparison of the pressure in the producer and injector well for different schemes

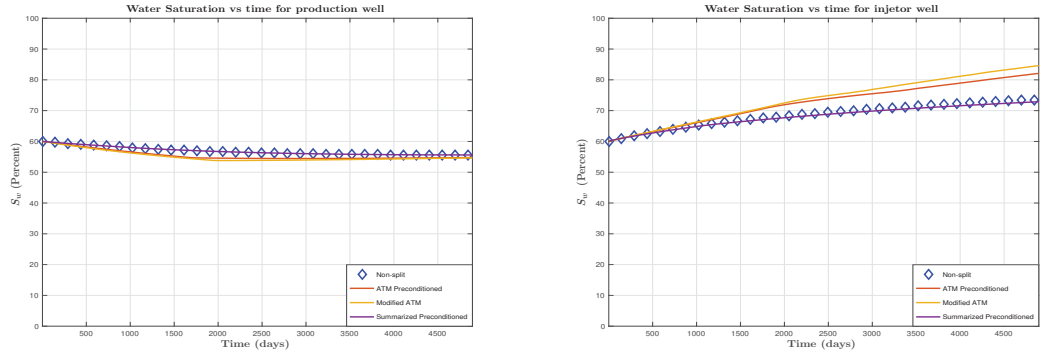

Figure 6.3: Comparison of the water saturation in the producer and injector well for different schemes

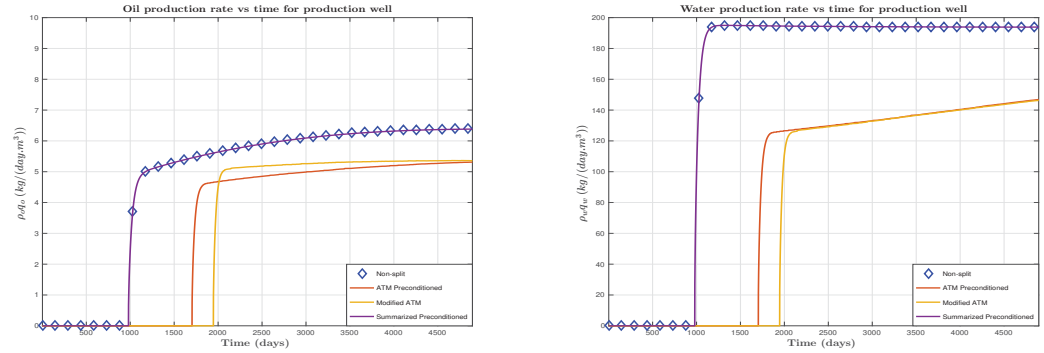

Figure 6.4: Comparison of oil and water production rate for different schemes

Chapter 7

Conclusion

7.1 Conclusion

We derived a preconditioned iterative scheme based on a summarized scheme which is unconditionally stable and first order accurate in time. We also derived two schemes based on the alternating triangle method, modified ATM iterative scheme and ATM preconditioned scheme, which are unconditionally stable but conditionally convergent. We conducted a numerical experiment to compare the two ATM schemes with the summarized preconditioned scheme. Our results demonstrated order of 1.2 for the summarized preconditioned scheme, order 2 for the modified ATM iterative scheme and order 1.5 for the ATM preconditioned scheme for the convergence of the pressure in time. They also showed that the summarized preconditioned iterative scheme performs better in terms of accuracy and efficiency. Also, it provided more reliable solutions than the solution from the ATM schemes. Both proposed schemes of the summarized preconditioned iterative scheme and the ATM schemes can be implemented on a parallel computer.

7.2 Future Topics

There are several future topics regarding our current work. The next phase of the project could be concentrated on flux-splitting schemes and upscaling.

The variation of permeability (K) in the pressure equation and the thermal conductivity (k_t) in energy equation usually occur at a scale much smaller than the physical domain of the problem. The ratio of scales is so small that it is expensive to computationally obtain pressure with the same resolution as what is given for the permeability. Thus, it becomes important to find optimal approximations at a scale much coarser, while somehow upscaling the given permeability information from the fine scale. Since pressure and temperature are parabolic their resolution on fine-scale, resolving the variation in the coefficient, is very time consuming. Thus, we have to apply a multi-scale technique to the pressure and the temperature equation.

The goal will be to explore the idea proposed in [22] called flux-splitting scheme. The scheme is based on an old but interesting idea for solving parabolic problems with highly heterogeneous coefficients. In the scheme, flux (directional derivatives) is considered as an independent variable. This results in a system of PDEs that yields not only the solution to the parabolic equation but also its flux. The flux-splitting scheme introduces a multi-scale method while naturally split the PDE for the flux. After solving for the flux directly, the desired solution to the parabolic equation is recovered knowing the value of the flux.

To demonstrate how the flux-splitting scheme will lead to the construction of the multi-scale method, we apply the scheme to the pressure equation (2.24)

for two-phase flow in section 4.2. We rewrite (2.24) in the following form:

$$\frac{\partial P}{\partial t} = \nabla.\Big(\frac{1}{CP_c}\Big(\Lambda_t \nabla P + \eta(\Lambda_w + \beta^{-1}\alpha\Lambda_o)\nabla z\Big)\Big) + \frac{\zeta(1+\omega)}{CP_c},\ \forall(\boldsymbol{x},t) \in \Omega \times \mathbb{R}^+$$

$$P(\boldsymbol{x},0) = P_0(\boldsymbol{x})$$

$$\Big(\frac{1}{CP_c}\Big(\Lambda_t \nabla P + \eta(\Lambda_w + \beta^{-1}\alpha\Lambda_o)\nabla z\Big)\Big).\mathbf{n} = 0, \qquad \forall \boldsymbol{x} \in \partial\Omega \tag{7.1}$$

where $\mathbf{n}$ denotes the (typically exterior) normal to the boundary $\partial\Omega$. Heterogeneity of the permeability data on fine grid and time dependencies through saturation are appeared through coefficients Λ_t, Λ_w, and Λ_o in the flux. We consider the flux as an independent variable by setting,

$$\frac{1}{CP_c}\Big(\Lambda_t \nabla P + \eta(\Lambda_w + \beta^{-1}\alpha\Lambda_o)\nabla z\Big) = \boldsymbol{v}, \tag{7.2}$$

in 2D, $\boldsymbol{v} = (v_1, v_2)$. We obtain a PDE governing the flux by substituting (7.2) into (7.1) and taking the gradient of the equation (7.1):

$$\frac{\partial}{\partial t}\left(\frac{CP_c\boldsymbol{v}}{\Lambda_t}\right) - \frac{\partial}{\partial t}\left(\frac{\eta\left(\Lambda_w + \beta^{-1}\alpha\Lambda_o\right)\nabla z}{\Lambda_t}\right) = \nabla\left(\nabla.\boldsymbol{v}\right) + \nabla f, \tag{7.3}$$

where $f(P, S_w) = \dfrac{\zeta\left(1+\omega\right)}{CP_c}$. Time derivative in first term of (7.3) can be computed by chain rule as:

$$\frac{\partial}{\partial t}\left(\frac{CP_c\boldsymbol{v}}{\Lambda_t}\right) = CP_c\left(\frac{1}{\Lambda_t}\frac{\partial \boldsymbol{v}}{\partial t} + \boldsymbol{v}\frac{\partial}{\partial t}\left(\frac{1}{\Lambda_t}\right)\right).$$

We denote $F(S_w) = \dfrac{1}{\Lambda_t}$, and $G(S_w) = \left(\dfrac{\eta\left(\Lambda_w + \beta^{-1}\alpha\Lambda_o\right)\nabla z}{\Lambda_t}\right)$ then the PDE

governing the flux in 2D becomes:

$$\begin{aligned}\left(\frac{CP_c}{\Lambda_t}\right)\frac{\partial v_1}{\partial t}+CP_c\ v_1\ \frac{\partial F}{\partial t}-\frac{\partial G}{\partial t}&=\frac{\partial^2 v_1}{\partial x\partial x}+\frac{\partial^2 v_2}{\partial x\partial y}+\frac{\partial f}{\partial x},\\ \left(\frac{CP_c}{\Lambda_t}\right)\frac{\partial v_2}{\partial t}+CP_c\ v_2\ \frac{\partial F}{\partial t}-\frac{\partial G}{\partial t}&=\frac{\partial^2 v_1}{\partial y\partial x}+\frac{\partial^2 v_2}{\partial y\partial y}+\frac{\partial f}{\partial y}.\end{aligned}\tag{7.4}$$

The novelty and main advantage of this formulation is that heterogeneous coefficients Λ_t, Λ_w, and Λ_o which varies on the fine scale is no longer a challenge since they are not acted on by a divergence operator which simplifies the construction of the multi-scale spatial discretization. We substitute (7.2) into the pressure equation (7.1) to get a pressure equation in terms of new variable, $\boldsymbol{v}$:

$$\frac{\partial P}{\partial t}=\nabla.(\boldsymbol{v})+f.\tag{7.5}$$

We discretize equations (7.4) and (7.5) in time by introducing $t^n=n\tau, n=0,1,...$ and denote approximation of $y(t^n)$ by y^n. Since F, and G are functions of the unknown saturation from equation (2.25) and their time discretization requires their evaluation at S_w^{n+1}, we must linearize the equations (7.4). We do linearization by simple iteration treatment. For example in this treatment, $F(S_w)$ at t^{n+1} is evaluated one iteration behind the desire solution, that is $F^{n+1}\approx F^{n+1,k}=F(S_w^{n+1,k})$, where k denotes iteration level. This requires coupling of saturation equation (2.25) with equations (7.4) and (7.5) as we see below. Then temporal discretization of the equations reads as: starting from a given $(v_1^0, v_2^0, P^0, S_w^0)$, we solve for the following problems to get

$\left(v_1^{n+1}, v_2^{n+1}, P^{n+1}, S_w^{n+1}\right)$ for $n = 1, 2, \cdots$.

$$\left(\frac{CP_c}{\Lambda_t^n}\right)\frac{v_1^{n+1,k+1}-v_1^n}{\tau}+CP_c\ v_1^{n+1,k+1}\ \frac{F^{n+1,k}-F^n}{\tau}-\frac{\partial^2 v_1^{n+1,k+1}}{\partial x\partial x}= \frac{G^{n+1,k}-G^n}{\tau}+\frac{\partial^2 v_2^{n+1,k}}{\partial x\partial y}+\frac{\partial f^{n+1,k}}{\partial x}, \tag{7.6a}$$

$$\left(\frac{CP_c}{\Lambda_t^n}\right)\frac{v_2^{n+1,k+1}-v_2^n}{\tau}+CP_c\ v_2^{n+1,k+1}\ \frac{F^{n+1,k}-F^n}{\tau}-\frac{\partial^2 v_2^{n+1,k+1}}{\partial y\partial y}= \frac{G^{n+1,k}-G^n}{\tau}+\frac{\partial^2 v_1^{n+1,k}}{\partial y\partial x}+\frac{\partial f^{n+1,k}}{\partial y}, \tag{7.6b}$$

$$\frac{P^{n+1,k+1}-P^n}{\tau}=\frac{\partial v_1^{n+1,k+1}}{\partial x}+\frac{\partial v_2^{n+1,k+1}}{\partial y}+f^{n+1,k+1}, \tag{7.6c}$$

$$\phi\frac{S_w^{n+1,k+1}-S_w^n}{\tau}=\frac{\partial v_{w1}^n}{\partial x}+\frac{\partial v_{w2}^n}{\partial y}+g^{n+1,k+1}, \tag{7.6d}$$

where $\boldsymbol{v_w} = (v_{w_1}, v_{w_2})$ is the flux of the saturation equation and it is related to the flux $\boldsymbol{v}$ in (7.2) through the relation:

$$\boldsymbol{v_w} = \Lambda_w\nabla P+\eta\Lambda_w\nabla z=\frac{CP_c\boldsymbol{v}-\eta\left(\Lambda_w+\beta^{-1}\alpha\Lambda_o\right)\nabla z}{\Lambda_t}\Lambda_w+\eta\Lambda_w\nabla z, \tag{7.7}$$

where

$$f^{n+1,k} = f(P^{n+1,k}, S_w^n),$$
$$f^{n+1,k+1} = f(P^{n+1,k+1}, S_w^n),$$
$$g^{n+1,k+1} = \zeta(P^{n+1,k+1}, S_w^n).$$

For spatial discretization, in 2D, we assume that $\Omega = (0, L_1) \times (0, L_2)$ is partitioned into N_1N_2 squares of size $H = L_1/N_1 = L_2/N_2$. The cell centres of these subdomains have coordinates (x_I^c, y_J^c), with $x_I^c = (I - 1/2)H, y_J^c =$

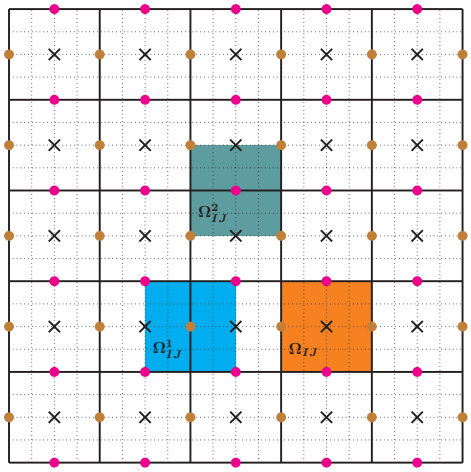

Figure 7.1: The MAC grid demonstrating finite volume Ω_{IJ} and co-volumes Ω^1_{IJ} and Ω^2_{IJ}

$(J-1/2)H, I = 1,\ldots,N_1; J = 1,\ldots,N_2$. (see figure 7.1 for staggered grid representation). These cells denoted by Ω_{IJ} construct the coarse partitioning of the domain Ω_H. The flux components v_1 and v_2 are collocated at the face-centres (x^f_I, y^c_J), with $x^f_I = (I-1)H, y^c_J = (J-1/2)H, I = 1,\ldots,N_1+1; J = 1,\ldots,N_2$ and (x^c_I, y^f_J), with $x^c_I = (I-1/2)H, y^f_J = (J-1)H, I = 1,\ldots,N_1; J = 1,\ldots,N_2+1$ correspondingly.

Denote Ω^i_{IJ} to be the co-volume corresponding to the flux component v_i. Ω^1_{IJ} and Ω^2_{IJ} will have sizes $H \times H$ with centres at $(x^f_I, y^c_J), I = 2,\ldots,N_1; J = 1,\ldots,N_2$ and $(x^c_I, y^f_J), I = 1,\ldots,N_1; J = 2,\ldots,N_2$ respectively.

Denote fine scale partitioning Ω_h by dividing each coarse-grid cell in Ω_H into $2n \times 2n$ cells of size $h = H/2n$ such that that the grid boundaries of the co-volumes coincide with those of the fine scale partition. This fine-scale partitioning is the scale that heterogeneity of the permeability occurs.

We can get the upscaled approximation on Ω_H by integrating (7.6a), (7.6b) and (7.6c) over Ω^1_{IJ}, Ω^2_{IJ} and Ω_{IJ} respectively. The saturation equation (7.6d) is discretized in space on the fine grid by integrating it over Ω_h after updating

$\boldsymbol{v}$ from coarse-scale in (7.6a), and (7.6b). Then we interpolate to get $\boldsymbol{v}$ for the underlying fine grid and then we obtain $\boldsymbol{v}_w$ from (7.7) on the fine grid.

$$\int_{\Omega_{IJ}^1} \left(\left(\frac{CP_c}{\Lambda_t^n} \right) \frac{v_1^{n+1,k+1} - v_1^n}{\tau} + CP_c \; v_1^{n+1,k+1} \; \frac{F^{n+1,k} - F^n}{\tau} - \frac{\partial^2 v_1^{n+1,k+1}}{\partial x \partial x} \right) d\Omega =$$

$$\int_{\Omega_{IJ}^1} \left(\frac{G^{n+1,k} - G^n}{\tau} + \frac{\partial^2 v_2^{n+1,k}}{\partial x \partial y} + \frac{\partial f^{n+1,k}}{\partial x} \right) d\Omega, \tag{7.8a}$$

$$\int_{\Omega_{IJ}^2} \left(\left(\frac{CP_c}{\Lambda_t^n} \right) \frac{v_2^{n+1,k+1} - v_2^n}{\tau} + CP_c \; v_2^{n+1,k+1} \; \frac{F^{n+1,k} - F^n}{\tau} - \frac{\partial^2 v_2^{n+1,k+1}}{\partial y \partial y} \right) d\Omega =$$

$$\int_{\Omega_{IJ}^2} \left(\frac{G^{n+1,k} - G^n}{\tau} + \frac{\partial^2 v_1^{n+1,k}}{\partial y \partial x} + \frac{\partial f^{n+1,k}}{\partial y} \right) d\Omega, \tag{7.8b}$$

$$\int_{\Omega_{IJ}} \left(\frac{P^{n+1,k+1} - P^n}{\tau} \right) d\Omega = \int_{\Omega_{IJ}} \left(\frac{\partial v_1^{n+1,k+1}}{\partial x} + \frac{\partial v_2^{n+1,k+1}}{\partial y} + f^{n+1,k+1} \right) d\Omega, \tag{7.8c}$$

$$\int_{\Omega_h} \left(\phi \frac{S_w^{n+1,k+1} - S_w^n}{\tau} \right) d\Omega = \int_{\Omega_h} \left(\frac{\partial v_{w1}^n}{\partial x} + \frac{\partial v_{w2}^n}{\partial y} + g^{n+1,k+1} \right) d\Omega. \tag{7.8d}$$

Applying the Gauss divergence theorem will simplify the terms containing second-order derivatives.

We will use the mid-point rule to evaluate $\int_{\Omega_{IJ}^i} \left(\frac{CP_c}{\Lambda_t^n} \right) \frac{v_i^{n+1,k+1} - v_i^n}{\tau}$ and $\int_{\Omega_{IJ}^i} CP_c v_i^{n+1,k+1} \; \frac{F^{n+1,k} - F^n}{\tau}$ in which Λ_t^n and $\frac{F^{n+1,k} - F^n}{\tau}$ are evaluated by the mid-point rule on the underlying fine grid in Ω_{IJ}^i. Again, we use the

mid-point rule on the underlying fine grid in Ω_{IJ}^i to evaluate $\int\limits_{\Omega_{IJ}^i} \frac{G^{n+1,k} - G^n}{\tau}$. We sample the source $f^{n+1,k+1}$ at the cell-centres of Ω_{IJ}, while $\frac{\partial f^{n+1,k}}{\partial x}$ and $\frac{\partial f^{n+1,k}}{\partial y}$ are integrated by the mid-point rule after approximation by central difference after integration by parts is applied. $g^{n+1,k+1}$ is sampled at the cell-centres of Ω_h. In the x direction, a Dirichlet boundary condition $v_1 = 0$, and in the y direction, a Dirichlet boundary condition $v_2 = 0$ are imposed following from the homogeneous Neumann boundary condition in (7.1). The spatial discretization (7.8a) and (7.8b) gives a tridiagonal system which in turn is very easy to solve by a direct solver. After solving for v_1 and v_2, we solve for P from (7.8c) then we interpolate to get $\boldsymbol{v}$ on the underlying fine grid and then we obtain $\boldsymbol{v}_w$ from (7.7) on the fine grid and we solve for S_w on the fine grid from (7.8d) explicitly at each iteration within each time step.

We note that the main purpose of flux-splitting scheme is two-fold: first, the heterogeneous coefficients which varies on a fine scale are no longer under the divergent operator. Second, the scheme (7.8a)-(7.8b) requires only solution of semi-discrete one-dimensional equations in each direction and this simplifies the construction of the multi-scale spatial discretization. The generalization to higher-dimensional problems is straightforward. Thereafter the above upscaling procedure in the framework of the compositional model can be applied.

Bibliography

[1] K. Aziz and A. Settari. *Petroleum Reservoir Simulation*. Applied Science Publishers Ltd., London, 1979.

[2] Z. Chen, G. Huan, and Y. Ma. *Computational Methods for Multiphase Flows in Porous Media*. SIAM, 2006.

[3] M. A. Christie and M. J. Blunt. Tenth spe comparative solution project: A comparison of upscaling techniques. *SPE*, pages 308–317, 2001.

[4] CMG. *User's Guide STARS, Advanced process and thermal reservoir simulator*. Computer Modelling Group Ltd., 2010.

[5] C. Dong. *An Integrated Multi-component Reservoir-wellbore Thermal Model*. PhD thesis, University of Calgary, 2012.

[6] J. Douglas, Jr., D. W. Peaceman, and H. H. Rachford, Jr. A method for calculating multi-dimensional immiscible displacement. *Trans. SPE AIME*, 222:297–306, 1959.

[7] J. Douglas, Jr. and H. H. Rachford, Jr. On the numerical solution of heat conduction problems in two and three space variables. *Transactions of the American Mathematical Society*, 82:421–439, 1956.

[8] M. Dusseault. Comparing venezuelan and canadian heavy oil and tar sands. In *the Petroleum Society's Canadian International Petroleum Conference*, pages 12–14, 2001.

[9] M. Islam, S. H. Mousavizadegan, S. Mustafiz, and J. H.Abou-Kasem. *Advanced Petroleum Reservoir Simulation*. John Wiley, 2010.

[10] W. Kwok. *Scalable linear and nonlinear algorithms for multiphase flow in porous media*. PhD thesis, Stanford University, 2007.

[11] H. P. Langtangen and G. K. Pedersen. *Scaling of Differential Equations*. Springer, 2016.

[12] G. I. Marchuk. Splitting and alternating direction methods. *Handbook of Numerical Analysis*, 1:197–462, 1990.

[13] P. D. Minev and C. R. Ethier. A characteristic/finite element algorithm for the 3-d Navier-Stokes equations using unstructured grids. *Computer Methods in Applied Mechanics and Engineering*, 178:39–50, 1999.

[14] D. W. Peaceman. *Fundamentals of Numerical Reservoir Simulation*. Elsevier, New York, 1977.

[15] D. W. Peaceman. Presentation of a horizontal well in numerical reservoir simulation. In *The 11th SPE Symposium on Reservoir Simulation*. SPE 21217, 1991.

[16] D. W. Peaceman and H. H. Rachford, Jr. The numerical solution of parabolic and elliptic differential equations. *J of SIAM*, 3:28–41, 1955.

[17] J. W. Sheldon, B. Zondek, and W. Cardwell. One-dimensional, incompressible, non-capillary, two-phase fluid flow in a porous medium. *Trans. SPE AIME*, 216:290–296, 1959.

[18] A. A. Smarskii. *An economical algorithm for the numerical solution of differential and algebraic equations. Zh. Vychisl. Mat. Mat. Fiz. 4(3), 580585.* in Russian, 1964.

[19] A. A. Smarskii. *The Theory of Difference Schemes.* Marcel Decker, New York, 2001.

[20] A. A. Smarskii, P. P. Matus, and P. N. Vabishchevich. *Differencee Schmes with Operator Factors.* Kluwer Academic Pub, 2002.

[21] H. L. Stone and A. O. Garder, Jr. Analysis of gas-cap or dissolved-gas reservoirs. *Trans. SPE AIME*, 222:92–104, 1961.

[22] P. N. Vabishchevich. Flux-splitting scheme for parabolic problems. *Computational Mathematics and Mathematical Physics*, 52:1128–1138, 2012.

[23] P. N. Vabishchevich. *Additive Operator-Difference Schemes. Splitting Schemes.* De Gruyer, 2014.

[24] P. N. Vabishchevich. Explicit schemes for parabolic and hyperbolic equations. *Applied Mathematics and Computation*, 250:424–431, 2015.

[25] N. N. Yanenko. *The method of Fractional Steps, The solution of problems of mathematical physics in several variables.* Springer, 1971.